Revealing Non-circular beam effect in WMAP-7 CMB maps with BipoSH measures of Statistical Isotropy

Nidhi Joshi[1,2], Santanu Das[2], Aditya Rotti[2], Sanjit Mitra[2] and Tarun Souradeep[2]
[1] *Centre for Theoretical Physics, Jamia Millia Islamia, New Delhi 110025, India*[*] *and*
[2] *IUCAA, Post Bag 4, Ganeshkhind, Pune-411007, India*[†]

arXiv:1210.7318v1 [astro-ph.CO] 27 Oct 2012

Mild, unavoidable deviations from circular-symmetry of instrumental beams in current Cosmic Microwave Background (CMB) experiments now pose a significant challenge to deriving high precision inferences from the high sensitivity and resolution of CMB measurements. It is important to be able to measure and characterize this subtle effect since it has bearing all subsequent inferences, including the cosmological parameters. We present analytic results, verified by numerical simulations, that CMB maps of cosmological signal that respect underlying statistical isotropy (SI) symmetry, measured with an instrument that has mildly non-circular (NC) beam would, nevertheless, exhibit SI violation. *Further, we show that appropriate observable measures constructed within the Bipolar spherical harmonic (BipoSH) representation of SI violation capture subtle NC-beam effects coupled with the scan strategy of the instrument.*

Accompanying their latest 7-year data release, the WMAP team published very high significance measurements of non-zero BipoSH spectra, $A^{20}_{\ell\ell}$ and $A^{20}_{\ell-2\ell}$, in the "W" and "V" band of the experiment. The BipoSH measurements at the two frequency channels show significant differences that point against an origin in the achromatic cosmological CMB anisotropy signal. We present a strong case that the BipoSH measurement are primarily explained by the quadrupolar ($m = 2$) component of the NC-beams, b_{l2}, of the respective channels. *The fact that subtle levels of non-circularity, e.g., WMAP beams* $|b_{l2}|/b_{l0} \lesssim 0.01$*, lead to measurable BipoSH spectra points to the immense promise and potential of the BipoSH representation.* We recover non-trivial qualitative features of the measured BipoSH spectrum that may be difficult to mimic through other effects. The scan strategy of CMB experiments, typically, employ multiple visits with varying orientation at different sky positions. Hence, the effective smoothing associated with the NC part of the beam is not expected to be represented by the raw NC-beam map. In general, the effective beam at any point will also have variations over the sky. The key result of this work is that using BipoSH measurements it is possible to estimate an equivalent single hit,'parallel transported' *effective* NC-beam that matches both the angular power spectrum and the non-zero BipoSH measurements of the observed maps. Hence, BipoSH analysis provides a very simple and effective characterization of CMB maps made with NC-beam. Last, but not the least, we successfully characterize an important systematic effect that limits all attempts to probe the SI assumption implied in the cosmological principle at high precision through CMB measurements beyond the angular power spectrum.

I. INTRODUCTION

Cosmic Microwave Background (CMB) experiments with high sensitivity, fine angular resolution covering almost the full sky have reached a point where even mild, unavoidable, deviations from circularity of the instrumental beam around its pointing direction poses a challenging systematic effect that must be overcome within finite computational resources to fully realize potential of these measurements for precision cosmology.

The effect of non-circular (NC) beam on angular power spectrum of CMB has been studied in literature and the non-trivial impact on high precision cosmological inferences has been appreciated but not satisfactorily resolved, particularly, within available computational resources. A significant body of literature attempting to deal with NC beam effect on the angular power spectrum exists, E.g., [1–8]. Further, the beam response function can acquire an inherent time dependence which complicates and hinders the deconvolution enormously. Consequently, beam imperfections, coupled with the scan strategy, lead to very complex modification of the signal demanding high computational resources to assess the final effect on the estimation of angular power spectrum and the cosmological parameters.

It is important to be able to capture the NC-beam effect in observed CMB maps. We provide a computationally efficient characterization of the NC-beam effect by focusing on its effect beyond the angular power spectrum. Beyond the angular power spectrum, the improvement in quality of CMB measurements now allow observational confrontation

[*]Electronic address: nidhijoshi@ctp-jamia.res.in
[†]Electronic address: santanud@iucaa.ernet.in aditya@iucaa.ernet.in sanjit@iucaa.ernet.in tarun@iucaa.ernet.in

of simplifying, theoretical, assumptions implicit in current cosmology. Given CMB fluctuations are a realization of correlated, Gaussian random field, the two point correlation function uniquely describes the statistics of the fluctuations. SI implies rotational invariance of the two point correlation function. Breakdown of SI can be parametrized by the expansion coefficients of the two point correlation function in Bipolar spherical harmonic (BipoSH) basis known as BipoSH coefficients. Cosmological CMB temperature fluctuations are generally assumed to be a realization of SI, Gaussian, correlated, random field on the sphere, consequently, the angular power spectrum has been the primary observational target of most CMB experiments. However, current and upcoming CMB experiments also hold the promise to observationally constrain the underlying, often implicit, SI assumption (closely linked to the so called, 'cosmological principle') employed in cosmology.

Statistical isotropy (SI) assumption underlying modern cosmology has been under intense scrutiny with hints of various 'anomalies' persisting in successive years of WMAP data [9–13]. Violation of SI can be generated both, from theoretically motivated possibilities such as, cosmic topology, anisotropic cosmologies etc. as well as from observational artifacts, such as, beam non circularity, anisotropic noise, foreground residuals, etc. [14–23]. Searching for the most plausible candidate of SI violation is a non trivial endeavor which strongly depends on observational and theoretical hints to narrow down the the possibilities. *While NC-beam effects do pose as a serious systematic contaminant for SI measurements, we demonstrate that the BipoSH representation measures of SI violation are also extremely effective in capturing, characterizing, and possibly, isolating subtle NC-beam effect in CMB maps.*

The recent detection of a quadrupolar power asymmetry 'anomaly' in WMAP 7 year data (WMAP-7) by the WMAP team using BipoSH representation measures [24] has proved to be an intriguing observation, that is yet to be satisfactorily explained. The published detections were significant both in the V-Band and W-Band frequency maps. Due to mildly significant differences in the BipoSH signal at the two frequencies and the fact that the signal seems to exhibit azimuthal symmetry in the ecliptic coordinate, it was suspected not to be of cosmological origin. Effects of residual galactic foreground emission would, arguably, be expected to be associated symmetries in the Galactic coordinate.

Observed CMB anisotropy (and polarization) on the sky are a convolution of the underlying cosmological CMB signal with the instrumental beam response function. The instrumental beams in most CMB experiments are nearly circularly (azimuthal) symmetric, but mild NC deviations do arise due unavoidable limitations in instrumental design, function and fabrication, e.g., the primary lobe of the beam exhibits non circularity due to the off-axis position of detectors on the focal plane, diffraction around the edges of instrument leads to side lobes of the beam, due to finite response time of detectors the scan may not correspond to the instrument rotating around its beam axis leading to the effective beam response at any pointing direction being sensitive to the scan strategy, etc.. *Regardless of the specific origin of non circularity in the beam response function, the key common point is the potentially measurable SI violation generated in the observed CMB maps.* It has been argued whether the non-circular beam effect in WMAP provides a plausible explanation of the observed non-zero BipoSH measurements [25, 26]. This paper presents the first results from a research program to directly assess the nature and amplitude of SI violation that can arise due to NC-beam response within the BipoSH representation and its implication for the WMAP-7 BipoSH 'anomaly'.

In the absence of symmetries, NC-Beam functions can be most generally expanded in BipoSH basis and coefficients of the expansion, $B^{LM}_{l_1 l_2}$, are referred to as *beam-BipoSH*. An ideal, circular symmetric beam ensures vanishing beam-BipoSH for all $L > 0$. Importantly, the beam-BipoSH at $L > 0$ not only capture NC-beam shape but also include the additional modulation arising from the specific scan strategy that sets the orientation of the NC-beam at any pixel. We show that every non-zero beam-BipoSH coefficient, $B^{LM}_{l_1 l_2}$, would generate a corresponding non-zero CMB BipoSH coefficient, $A^{LM}_{l_1 l_2}$, in the observed CMB map.

The analytic formulation presented is valid for any arbitrary beam shape but progress to explicit expressions is possible within an idealized 'parallel-transport' (PT) scan strategy approximation [1]. Further, mild deviations from circular symmetry, that permit a perturbative approach, and residual, discrete even-fold azimuthal, symmetry in the NC beam imply that the analytic results at the leading order quadrupolar-non-circularity ($m = 2$) are sufficient for the present observations. At the leading order of our approximations, we provide simple explicit analytic expressions only for BipoSH coefficients due to *mildly* NC-beams that retain *discrete even-fold azimuthal and reflection* symmetry relevant to explaining the WMAP-7 BipoSH results. Assuming reflection-symmetric beam function restricts the set to even parity BipoSH coefficients [45]. The published WMAP BipoSH results claim that in ecliptic coordinates BipoSH at $(L = 2, M = 0)$ are the non-zero BipoSH measured. Our general analytic formulation then suggests that a PT-scan [1]) approximation should be fairly good simplifying approximation for the WMAP scan for the dominant $m = 2$ mode of NC-beams in the ecliptic coordinates. We support this assertion with maps quantifying the departures from this approximation for a realistic WMAP scan. Further, the multiple hits of the beam with varying orientation at any pixel would tend to reduce (average out) the level of non-circularity significantly. In particular, it can be estimated in the specific case of WMAP scan, the $m = 2$ mode, b_{l2}, in the raw NC-beam can be expected to reduce by about a factor of ~ 0.5, and higher m modes maps are expected to suffer even progressively greater reduction. However, we also show analytically that scaling will have a dependence on the multipole, l, that is, in principle, computable given

detailed scan information including multiple visits and corresponding orientation at all the sky pixels.

Assuming that the entire BipoSH signal measured by WMAP arises due to NC-beam effect, we determine spectrum of quadrupolar ($m = 2$) mode, $b_{l2}^{\rm eff}$, of an effective beam (incorporating multiple visits by the beam to sky pixels) that fits the measured BipoSH spectra. We fit for a constant rescaling of the raw beam $b_{l2}^{\rm eff} = \alpha b_{l2}$. Although, the best-fit $\alpha \sim 0.4$ obtained matches our expectation, the reduced χ^2 of the fit is unsatisfactory, and would, at best, explain part of the BipoSH signal. We find that a linear l dependent correction to a constant scaling, $b_{l2}^{\rm eff} = (\alpha + \beta \cdot l) b_{l2}$ lead to very good fit to the measured WMAP-7 BipoSH spectra. We provide analytic understanding of the l-dependent scaling, f_l. The linear fit explored is a simple 'phenomenological' fit to f_l. Detailed, computationally expensive numerical simulations incorporating the two beam differencing, real scan and map making may justify the linear correction to the constant scaling, or, lead to the conclusion that the entire BipoSH signal cannot be attributed to NC-beam leaving room for other uncorrected systematic effects, or even hint at cosmological SI violation.

We verify all analytic results and estimate error-bars through extensive numerical simulations of SI CMB maps scanned by real space convolution with corresponding NC-beam maps. The numerical simulations presented here are limited to the PT-scan, single side, NC-beam studied analytically. As explained later, without simplifying assumptions, realistic simulations using the WMAP beam differencing and scan are more compute intensive primarily because we find that the results are fairly sensitive to side lobe and other spread-out features (out to ~ 10 times the FWHM from the beam centre), present in the beam maps released by the WMAP team [27]. Hence, we defer the results from ongoing realistic simulations to a future publication.

The paper is arranged as follows. Sec. II provides a brief primer to the BipoSH formalism to characterize SI violations to keep the paper self contained. In Sec. III we present a novel expansion of the beam response function in the BipoSH basis, referred to as *beam-BipoSH* coefficients in the article. In Sec. IV we derive expressions for the CMB BipoSH coefficients arising from the convolution of SI CMB anisotropy signal with general NC-beams. We also provide the simpler explicit analytic expressions for beam-BipoSH coefficients for a mildly non-circular beam within the PT-scan approximation. As a test case, we study the Elliptical Gaussian NC-beam model that has minimal parameters with clear interpretation. The beam spherical harmonic transforms (*beam-SH*) have analytic expressions and permit simple, well controlled perturbative treatment of the NC-effects. We also use this case to test and qualify our numerical simulations against analytic results. In Sec. V, we get closer to addressing the WMAP-7 BipoSH measurements by first computing the BipoSH spectra based on the beam-SH of single-side, raw beam maps (Sec. V A). In Sec. V B we fit for parametrized scaling functions, f_l of the leading order raw beam-SH that would reproduce the WMAP-7 BipoSH spectra measurements as arising entirely from uncorrected NC beam effect. Sec. VI has discussions and presents the conclusions of this paper. Detailed steps of all analytical calculations are provided for completeness in Appendix A and B. Appendix C provides an analytic derivation of an effective beam arising from multiple hits at varying orientations in terms of a rescaled beam-SH the raw beam map.

II. PRIMER: BIPOLAR SPHERICAL HARMONIC (BipoSH) REPRESENTATION

The CMB anisotropy signal is a random field on the surface of a sphere and can, hence, be expanded in the spherical harmonic (SH) basis,

$$\Delta T(\hat{n}) = \sum_{lm} a_{lm} Y_{lm}(\hat{n}) \,, \tag{1}$$

and equivalently represented in the set of random variables a_{lm}. Statistical properties of a random field are characterized by its n-point correlation function. Statistical isotropy implies expectation values of all N-point correlation functions are invariant under the rotations of the sky. The statistical distribution of fluctuations in temperature field are observationally consistent with Gaussian statistics. Hence, the two-point function $C(\hat{n}, \hat{n}') \equiv \langle \Delta T(\hat{n}) \Delta T(\hat{n}') \rangle$ is expected to completely encode all information pertaining to the CMB anisotropy, $\Delta T(\hat{n})$. For CMB sky respecting statistically isotropy (SI), the correlation function only depends on the angle between the two directions $\hat{n}_1$ and $\hat{n}_2$ and the two point function can then be expanded in Legendre polynomials, as

$$C(\hat{n}_1, \hat{n}_2) \equiv C(\hat{n}_1 \cdot \hat{n}_2) = \sum_l \frac{(2l+1)}{4\pi} C_l P_l(\hat{n}_1 \cdot \hat{n}_2), \tag{2}$$

where the coefficients of expansion C_l define the angular power spectrum. The random spherical harmonic moments, a_{lm} are then statistically independent leading to a diagonal covariance matrix in the SH basis,

$$\langle a_{lm} a^*_{l'm'} \rangle = C_l \delta_{ll'} \delta_{mm'} \tag{3}$$

which also implies that (the m-independent), C_l encodes all the information in a Gaussian, SI field on the full sky (complete sphere, $\mathbf{S}^2$). In general, SI violation leads to non-zero off-diagonal elements (for specific subset of SI violations, the SH covariance matrix remains diagonal, but m dependent). The two point correlation function, most generally, then depends on both the directions $\hat{n}_1$ and $\hat{n}_2$ and not just on the angle between them. The most convenient expansion basis for $C(\hat{n}_1, \hat{n}_2) \not\equiv C(\hat{n}_1 \cdot \hat{n}_2)$ is the Bipolar Spherical Harmonic(BipoSH) basis[28–33].

$$C(\hat{n}_1, \hat{n}_2) = \sum_{l_1, l_2, L, M} A^{LM}_{l_1 l_2} \{Y_{l_1}(\hat{n}_1) \otimes Y_{l_2}(\hat{n}_2)\}_{LM}, \tag{4}$$

where $A^{LM}_{l_1 l_2}$ are BipoSH coefficients and the bipolar spherical harmonic (BiPoSH) functions,

$$\{Y_{l_1}(\hat{n}_1) \otimes Y_{l_2}(\hat{n}_2)\}_{LM} = \sum_{m_1 m_2} C^{LM}_{l_1 m_1 l_2 m_2} Y_{l_1 m_1}(\hat{n}_1)\, Y_{l_2 m_2}(\hat{n}_2), \tag{5}$$

are irreducible tensor product of two spherical harmonics spaces that form an orthonormal basis on $\mathbf{S}^2 \times \mathbf{S}^2$ and, here, $C^{LM}_{l_1 m_1 l_2 m_2}$ are Clebsch-Gordon coefficients. The indexes of these coefficients satisfy the triangularity conditions $|l_1 - l_2| \leq L \leq l_1 + l_2$ and $m_1 + m_2 = M$. The transformation properties of BipoSH under rotations are similar to spherical harmonics [34].

The BipoSH coefficients can be shown to be linear combinations of off-diagonal elements of the harmonic space covariance matrix,

$$A^{LM}_{l_1 l_2} = \sum_{m_1 m_2} \langle a_{l_1 m_1} a^*_{l_2 m_2} \rangle (-1)^{m_2} C^{LM}_{l_1 m_1 l_2 - m_2}, \tag{6}$$

where a_{lm}'s are the spherical harmonic coefficients of the CMB maps [28]. The SI part given in Eq. (3), corresponds to $(L = 0, M = 0)$, since , $C^{00}_{lml'-m'} \propto \delta_{ll'}\delta_{mm'}$. *Non-zero BipoSH coefficients with $L > 0$ that capture SI violation also neatly encode the residual symmetries of the two point correlation function* [35]. The correlation function is always real and symmetric under the exchange of $\hat{n}_1$ and $\hat{n}_2$, reflected in the following symmetry properties for BipoSH coefficients,

$$A^{LM}_{l_1 l_2} = \begin{cases} (-1)^{l_1 + l_2 - L + M} A^{*L-M}_{l_1 l_2} \\ \\ (-1)^{l_1 + l_2 - L} A^{LM}_{l_2 l_1} \end{cases}. \tag{7}$$

As a consequence, BipoSH coefficients are always real if $M = 0$ and $l_1 + l_2 + L$ is even and always imaginary if $M = 0$ and $l_1 + l_2 + L$ is odd. If the observed CMB sky is statistically isotropic, it can be shown that all the BipoSH coefficients vanish except the coefficients of the form A^{00}_{ll} which can be expressed in terms of the CMB angular power spectrum [28],

$$A^{LM}_{l_1 l_2} = (-1)^{l_1} C_{l_1} \prod_{l_1} \delta_{l_1 l_2} \delta_{L0} \delta_{M0}, \tag{8}$$

where, for brevity, the standard notation $\prod_{ab\ldots c} = \sqrt{(2a+1)(2b+1)\ldots(2c+1)}$ is introduced and employed in the rest of this paper [34].

Recently it has also been realized that BipoSH space representation separates into two distinct classes,

- Even parity BipoSH coefficients $A^{LM(+)}_{l_1 l_2}$ where $l_1 + l_2 + L$ is even obey $A^{LM(+)*}_{l_1 l_2} = (-1)^M A^{L\,-M(+)}_{l_1 l_2}$, and
- Odd parity BipoSH coefficients $A^{LM(-)}_{l_1 l_2}$ with $l_1 + l_2 + L$ odd, obey $A^{LM(-)*}_{l_1 l_2} = (-1)^{M+1} A^{L\,-M(-)}_{l_1 l_2}$,

where the 'parity' terminology here is based on the analogy with parity transformation properties of ordinary spherical harmonic moments.

It is often easy to anticipate, or determine, the parity property of a possible cause of SI violation. This distinction then provides very valuable clues to the origin of SI violations e.g., weak lensing due to scalar (even parity) and tensor (odd parity) perturbations [36], anisotropic primordial power spectrum (even) [18], temperature modulation (even) [37], primordial homogeneous magnetic fields (even) [17, 38]. Importantly, in the context of origin of WMAP BipoSH measurements from NC-beam effect, the absence of significant odd parity BipoSH would justify the simple parallel-transport (PT) scan approximation adopted in our analytic approach.

III. Beam – BipoSH: NON-CIRCULAR BEAMS IN BipoSH REPRESENTATION

It is very important to characterize the non-circularity of the beam through appropriate measures. We show that NC-beam is clearly represented in BipoSH space. Beam response function characterizes the angular dependence of the sensitivity of the apparatus around the pointing direction $\hat{n}_1$. We expand the beam function around the pointing direction $\hat{n}_1$ in Spherical Harmonic (SH) basis as,

$$B(\hat{n}_1, \hat{n}_2) = \sum_{lm} b_{lm}(\hat{n}_1) Y_{lm}(\hat{n}_2). \tag{9}$$

The beam-SH coefficients when the beam is pointed at $\hat{n}_1$, are given by

$$b_{lm}(\hat{n}_1) = \int d\Omega_{\hat{n}_2} B(\hat{n}_1, \hat{n}_2) Y_{lm}(\hat{n}_2). \tag{10}$$

The SH transform of beam at arbitrary pointing direction, $\hat{n} \equiv (\theta, \phi)$ is given by *beam-SH*, $b_{lm'}(\hat{z})$ – the SH transform of the beam pointed along $\hat{z}$, the North pole [1],

$$b_{lm}(\hat{n}) = \sum_{m'} b_{lm'}(\hat{z}) D^l_{mm'}(\phi, \theta, \rho(\hat{n})), \tag{11}$$

where Wigner D-functions $D^l_{mm'}(\alpha, \beta, \gamma)$ are the matrix elements of the rotation operator ($0 \leq \alpha < 2\pi,\ 0 \leq \beta < \pi,\ 0 \leq \gamma < 2\pi$) and α, β, γ are the Euler angles that rotates the $\hat{z}$-axis to the pointing direction $\hat{n} = (\theta, \phi)$ and the angle $\rho(\hat{n})$ specifies the orientation of the NC-beam with respect to the local Cartesian ($\hat{x} \equiv \hat{\phi}, \hat{y} \equiv \hat{\theta}$) aligned with spherical coordinates [1]. Such a rotation can be realized by fixing a coordinate system and performing anti-clockwise rotations, first rotating about the $\hat{z}$-axis by an angle $\alpha = \phi$, then rotating about new $\hat{y}$-axis by an angle $\beta = \theta$, and finally about the new $\hat{z}$-axis by $\gamma = \rho(\hat{n})$. Rotation is such that the beam pointing direction, $\hat{n}$ and $\rho(\hat{n})$ is the relative orientation of the beam around its axis set by the the scan pattern of the experiment.

In this work we introduce a more general NC-beam characterization in the BipoSH representation. Since, a general NC-Beam function depends on two vector directions, it can be expanded in the BipoSH basis (see Sec. II) ,

$$B(\hat{n}_1, \hat{n}_2) = \sum_{l_1 l_2 LM} B^{LM}_{l_1 l_2} \sum_{m_1 m_2} C^{LM}_{l_1 m_1 l_2 m_2} Y_{l_1 m_1}(\hat{n}_1) Y_{l_2 m_2}(\hat{n}_2), \tag{12}$$

where the coefficients of expansion $B^{LM}_{l_1 l_2}$ are referred to as *beam-BipoSH* coefficients . As will be clear in the sections ahead, beam-BipoSH coefficients have the advantage of capturing the additional effect of scan strategy together with non-circularity of the beam.

The beam-BipoSH coefficient can be readily related to beam function in spherical harmonic basis ,

$$B^{LM}_{l_1 l_2} = \sum_{m_1 m_2} C^{LM}_{l_1 m_1 l_2 m_2} \int d\Omega_{\hat{n}} b_{l_2 m_2}(\hat{n}) Y^*_{l_1 m_1}(\hat{n})\,. \tag{13}$$

A circularly symmetric beam function around the pointing direction can be expanded in Legendre polynomials, $B(\hat{n}_1, \hat{n}_2) \equiv B(\hat{n}_1 \cdot \hat{n}_2) = (4\pi)^{-1} \sum_l (2l+1) B_l P_l(\hat{n}_1 \cdot \hat{n}_2)$. Inverse transforming Eq.(12) and using orthogonality of BipoSH[34], we obtain beam-BipoSH coefficients for circularly symmetric beam function,

$$B^{LM}_{l_1 l_2} = B_{l_1} \delta_{l_1 l_2} (-1)^{l_1} \prod_{l_1} \delta_{L0} \delta_{M0}, \tag{14}$$

where B_l is the commonly used Legendre transform of the beam function in the circularized beam approximation.

A. General expression for an arbitrary scan strategy

Using Eq. (11) and (13), it turns out that for any arbitrary scanning strategy, the beam-BipoSH can be expressed in terms of the beam-SH as,

$$B^{LM}_{l_1 l_2} = \sum_{m_1 m_2} C^{LM}_{l_1 m_1 l_2 m_2} \sum_{m'} b_{l_2 m'}(\hat{z}) \int_{\theta=0}^{\pi} \int_{\phi=0}^{2\pi} D^{l_2}_{m_2 m'}(\phi, \theta, \rho(\theta, \phi)) Y^*_{l_1 m_1}(\theta, \phi) \sin\theta d\theta d\phi. \tag{15}$$

To separate the azimuthal (ϕ) and polar (θ) dependencies, it is convenient to expressed Wigner-D functions in terms of Wigner-d through following relation,

$$D^l_{mm'}(\phi,\theta,\rho) = \mathrm{e}^{-im\phi}\, d^l_{mm'}(\theta)\, \mathrm{e}^{-im'\rho}. \tag{16}$$

Eq. (15) is the most general expression of beam-BipoSH coefficients for any given NC-beam specified through $b_{lm}(\hat{z})$ and scan pattern, defined by $\rho(\theta,\phi)$, in any spherical polar coordinate system. The beam-BipoSH coefficients can be evaluated numerically from the beam maps of the NC-beam. When the beam is circularly symmetric, $b_{lm}(\hat{z}) = B_l\sqrt{\frac{2l+1}{4\pi}}\delta_{m0}$, and it is straightforward to establish that Eq.(15) reduces to Eq.(14). Beam-BipoSH depend not only on NC-beam harmonics but also on the scan-strategy that defines $\rho(\hat{n})$. We motivate a particular idealized scan pattern where $\rho(\hat{n})$ is constant in a some coordinate system, that not only allows a completely analytic treatment but is also reasonably well-justified in the context of the BipoSH signature measured in WMAP-7. Analytic progress is far less tedious when the beam has mild deviations from circularity allowing a perturbative approach that retains only the leading order terms. We validate numerically that these approximations used are indeed fairly adequate for the explanation of the WMAP BipoSH measurements.

B. 'Parallel-transport' scan approximation

The general beam-BipoSH in Eq. (15) can be tackled analytically if when the scan pattern is such that $\rho(\hat{n})$ is a constant. *We refer to this case as 'parallel-transport' (PT) scan following [1].* The PT-scan approximation implies that the orientation of the beam relative to the local longitude is constant at any point on the sky. A beam response function with reflection symmetry will generate only real, non-vanishing beam-BipoSH coefficients. The leading order $m = 2$ dominates for a mildly NC-beam. For real coefficients only the $\cos(2\rho)$ part is important (see Eq.(15)). Fig. 1 shows the map for $\cos(2\rho)$ for a full year scan. For WMAP scan pattern, the constant ρ approximation for $m = 2$ holds good over the significant (blue) band around the equator in an ecliptic coordinate system. Therefore, for a fair fraction of the sky part of the map our constant ρ approximation for $m = 2$ mode of non-circularity is a fair assumption. The compute-intensive numerical comparison of results from this approximation with the real WMAP scan is underway and will be reported in the near future.

For constant $\rho(\hat{n}) \equiv \rho$, the orthogonality relation,

$$\int_{\phi=0}^{2\pi} \exp(-i(m_1+m_2)\phi)\, d\phi = 2\pi\, \delta_{m_1,-m_2}\,, \tag{17}$$

implies that the integral over ϕ in Eq.(15), will separate from the integral over θ and would restrict the non-zero beam-BipoSH to $M = 0$,

$$B^{LM}_{l_1l_2} = 2\pi\delta_{M0}\sqrt{\frac{(2l_1+1)}{4\pi}}\sum_{m'} b_{l_2m'}(\hat{z})\exp(-im'\rho)\sum_{m_2} C^{L0}_{l_1-m_2l_2m_2}\int_{\theta=0}^{\pi} d^{l_2}_{m_2m'}(\theta)d^{l_1}_{-m_20}(\theta)\sin\theta d\theta. \tag{18}$$

We define

$$I^{l_1l_2}_{m_2,m'} = (-1)^{m_2}\sqrt{\frac{(2l_1+1)}{4\pi}}\int d^{l_2}_{m_2m'}(\theta)d^{l_1}_{m_20}(\theta)\sin\theta d\theta. \tag{19}$$

Here we have used the symmetry property of Wigner-d functions, $d^l_{mm'} = (-1)^{m-m'}d^l_{-m-m'}$. Beam-BipoSH coefficients in the constant $\rho(\hat{n})$ approximation take the following form,

$$B^{LM}_{l_1l_2} = 2\pi\delta_{M0}\sum_{m'} b_{l_2m'}(\hat{z})\exp(-im'\rho)\sum_{m_2} C^{L0}_{l_1-m_2l_2m_2} I^{l_1l_2}_{m_2,m'}. \tag{20}$$

For a mildly non circular beam, the summation can be truncated at a low value of m'. Further, NC-beams that retains discrete even-fold azimuthal symmetry will have $b_{lm}(\hat{z}) = 0$ for odd values of m. In BipoSH space, the consequence of discrete even-fold azimuthal and reflection symmetric NC-beam translates to restricting non-zero beam-BipoSH to $M = 0$ and $l_1 + l_2 =$ even. Imposing reflection symmetry, beam-BipoSH are restricted to even values of multipole L. We derive explicit expressions for beam-BipoSH coefficients up to leading order ($m' = 2$) term .

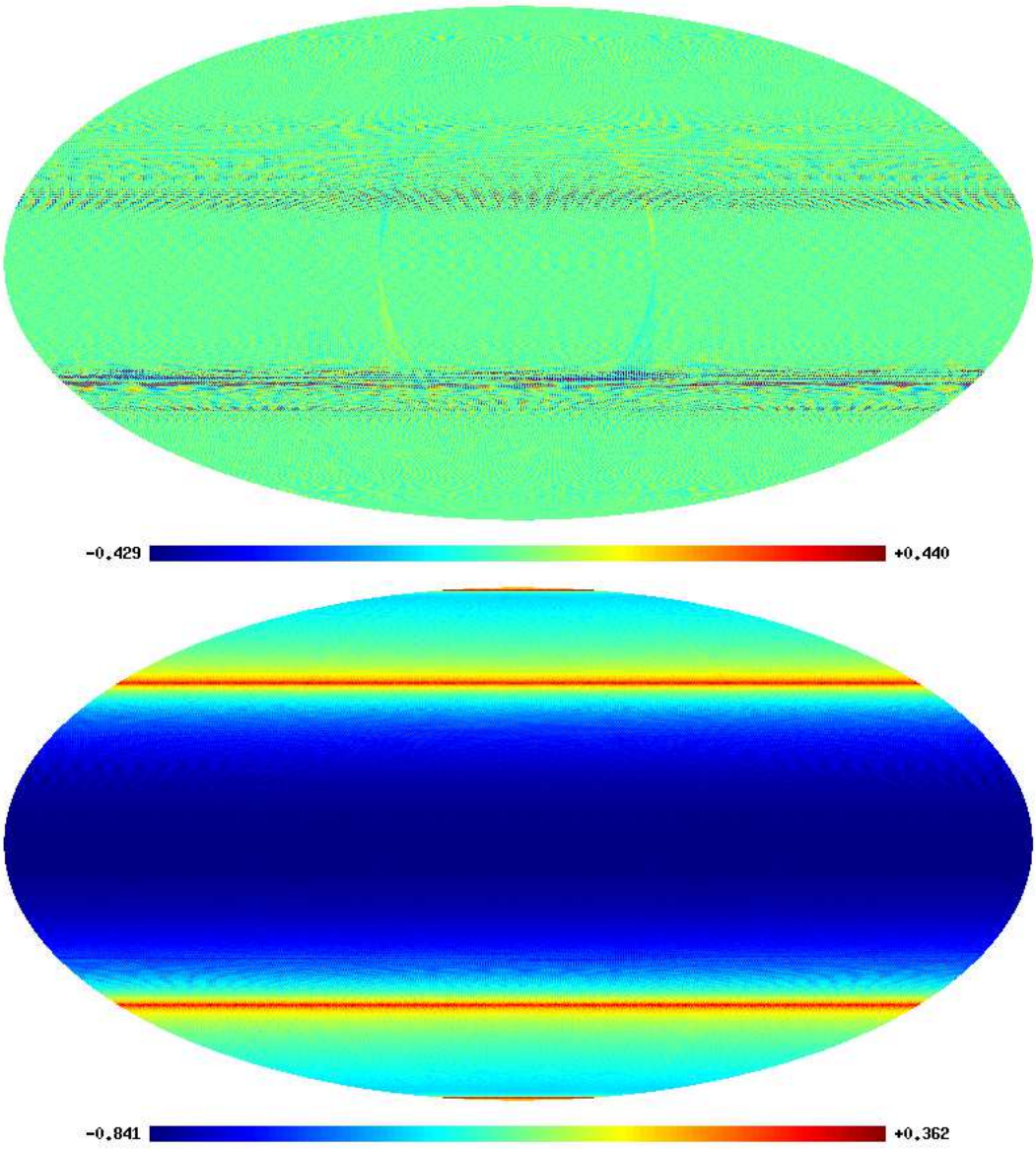

FIG. 1: *Top:* Map of $\bar{\rho}(\hat{n}) = [N(\hat{n})]^{-1} \sum_i \rho_i(\hat{n})$ defining the orientation of the beam averaged over multiple hits, $i = 1$ to $N(\hat{n})$ for numerically simulated one year of WMAP scan. At most pixels, $\bar{\rho}(\hat{n})$ averages to a value close to zero. However, it also shows a very intricate fine patterns of small regions with marked deviation from zero. *Bottom:* Map of $\cos(2\bar{\rho})$ in ecliptic coordinates for full year WMAP scan provides a rough guide to the validity of the PT-scan approximation for the dominant $m = 2$ non-circularity for the WMAP scan strategy. Note that over a wide band of latitudes (blue region), the PT-scan approximation is roughly valid. Strong deviation are seen at and beyond the two latitude-symmetric thin bands (red) at moderately high latitudes in North and South hemispheres.

To make analytical progress, we need to evaluate $I^{l_1 l_2}_{m_2,m'}$ for $m' = -2, 0, 2$. It is important to note that, $m' = 0$ corresponds to the usual circular symmetric beam-BipoSH ($L = 0$) coefficient. The non-circular $m' = \pm 2$ will give rise to non-trivial (quadrupolar, $L = 2$) beam-BipoSH. For circular symmetric ($m' = 0$) beam-BipoSH (refer AppendixA),

$$I^{l_1 l_2}_{m_2,0} = (-1)^{m_2} \sqrt{\frac{(2l_1+1)}{4\pi}} \frac{2}{2l_2+1} \delta_{l_1 l_2}\,, \quad \forall m_2\,, \tag{21}$$

$$B^{LM}_{l_1 l_2} = (-1)^{l_2} b_{l_2 0}(\hat{z}) \sqrt{4\pi} \delta_{l_1 l_2} \delta_{L0} \delta_{M0} \delta_{m'0}. \tag{22}$$

For $m' = \pm 2$, the integrals are evaluated separately for the $m_2 = 0$ and $m_2 \neq 0$ parts of the summation. In the former

case when $m_2 = 0$ and $m' = \pm 2$, the integral

$$I^{l_1 l_2}_{0,\pm 2} = \sqrt{\frac{(2l_1+1)}{4\pi}} \begin{cases} 0 & \text{if } (l_1 + l_2 \equiv \text{odd}) \\ 0 & \text{if } (l_1 > l_2) \\ 4\sqrt{\frac{(l_2-2)!}{(l_2+2)!}} & \text{if } (l_1 < l_2) \\ \sqrt{\frac{(l_2-2)!}{(l_2+2)!}}\left[\frac{4l_2}{(2l_2+1)} - \frac{2l_2(l_2+1)}{(2l_2+1)}\right] & \text{if } (l_1 = l_2)\,. \end{cases} \tag{23}$$

For $m_2 \neq 0$, $d^{l_2}_{m_2 \pm 2}(\theta)$ is recursively expanded in terms of $d^{l_2}_{m_2 0}(\theta)$ to evaluate $I^{l_1 l_2}_{m_2,\pm 2}$ (refer Appendix A).

This work is motivated by the highly significant measurements of BipoSH published by the WMAP team [24]. Interestingly, the publication claimed that for the $L = 2$ BipoSH spectra measured are significantly non-zero only for $M = 0$ in the ecliptic coordinates. This has been independently confirmed by our BipoSH measurements on WMAP-7, as well. As shown in following Sec. IV, this implies that only beam-BiPoSH with $M = 0$ are relevant for understanding the WMAP BipoSH results. Consequently, it suggests that if NC-beam is responsible for non-zero BipoSH measurements, the WMAP scan pattern is such that, in ecliptic coordinate, $\rho(\hat{n}) \approx$ *constant* must be a good approximation for the dominant $m = 2$ mode of the NC beams of WMAP. This is being quantitatively assessed through more compute intensive, numerical simulations with realistic WMAP scan patterns (i.e., without invoking PT-scan approximation and incorporating map-making from actual two side difference measurement). We take advantage of the simplicity afforded in the PT-scan approximation to proceed to explicit analytic expressions that readily provide broader as well deeper insight than compute expensive numerical simulations.

This also implies that only even-parity beam-BipoSH would be relevant for our comparison to WMAP BipoSH results where the estimator used is by definition is strictly restricted even-parity BipoSH. Non circular beam with additional reflection symmetry restrict beam-BipoSH to even-parity,

$$B^{LM}_{l_1 l_2} \equiv B^{LM^{(+)}}_{l_1 l_2} = 2\pi\delta_{M0}\left(b_{l_2 2}(\hat{z})\mathrm{e}^{-i2\rho} + b^*_{l_2 2}(\hat{z})\mathrm{e}^{i2\rho}\right)\left[C^{L0}_{l_1 0 l_2 0} I^{l_1 l_2}_{0,2} + \sum_{m_2 \neq 0} C^{L0}_{l_1 - m_2 l_2 m_2} I^{l_1 l_2}_{m_2,2}\right]. \tag{24}$$

Refer to Appendix A for details. Note that a constant ρ can be absorbed as phase factor in the redefinition of the complex quantity $b_{lm}(\hat{z})$ essentially resetting the orientation of the beam when pointed at North pole. Hence, in the PT-scan approximation,

$$B^{LM^{(+)}}_{l_1 l_2} = 2\pi\delta_{M0}(b_{l_2 2}(\hat{z}) + b^*_{l_2 2}(\hat{z}))\big(C^{L0}_{l_1 0 l_2 0} I^{l_1 l_2}_{0,2} + \sum_{m_2 \neq 0} C^{L0}_{l_1 - m_2 l_2 m_2} I^{l_1 l_2}_{m_2,2}\,\big). \tag{25}$$

We emphasize that the above expression for beam-BipoSH coefficient hold for the PT-scan approximation (with constant $\rho(\hat{n})$) for a NC-beam that has reflection symmetry. Although we have restricted explicit analytic results presented in the text to reflection symmetric beam functions, in general, odd parity beam BipoSH will be non-vanishing in absence of the above mentioned symmetries. Appendix A provides expressions for odd-Parity beam-BipoSH, $B^{LM^{(-)}}_{l_1 l_2}$, that can be used as a measure of breakdown of reflection symmetry in NC beam[46]. Note that the BipoSH estimator [37], that differ by a factor from original definition of Hajian & Souradeep [28, 33], used by the WMAP team cannot be extended to odd-parity BipoSH, However, it is possible to devise BipoSH estimators that can measure odd-parity BipoSH spectra while matching that employed by WMAP for even-parity BipoSH spectra [39].

IV. NON-CIRCULAR BEAM IMPRINT ON BipoSH OF CMB MAPS

The observed CMB map is a convolution of the signal with the instrumental beam. Instrument beam response functions of all experiments have deviations from circular symmetry at some level. However, circular symmetric beam response function around the pointing direction is often assumed to simplify the analysis of the the beam effect. This key assumption does affect many stages of CMB data analysis and should be measured and characterized.

In this section we show that CMB maps made with non-circular beam exhibit statistical isotropy (SI) violation in an otherwise SI cosmological CMB signal. BipoSH coefficients have proved to be robust, model independent, measure of SI violation. Further, BipoSH representation provides clear insight into the nature and extent of the residual symmetry and parity [35, 36] and, hence, helps pin down the most plausible origin of SI violation.

The measured CMB temperature fluctuations map, $\widetilde{\Delta T}(\hat{n})$ is the convolution of true underlying CMB temperature fluctuations $\Delta T(\hat{n})$ with the instrument beam,

$$\widetilde{\Delta T}(\hat{n}_1) = \int d\Omega_{n_2} B(\hat{n}_1, \hat{n}_2) \Delta T(\hat{n}_2). \tag{26}$$

where the beam response function $B(\hat{n}_1, \hat{n}_2)$ gives the sensitivity of an experiment around the pointing direction. The observed two point correlation function will be,

$$\tilde{C}(\hat{n}_1, \hat{n}_2) \equiv \langle \widetilde{\Delta T}(\hat{n}_1) \widetilde{\Delta T}(\hat{n}_2) \rangle = \int d\Omega_n \int d\Omega_{n'} C(\hat{n}', \hat{n}) B(\hat{n}_1, \hat{n}') B(\hat{n}_2, \hat{n}), \tag{27}$$

where $C(\hat{n}', \hat{n}) = \langle \Delta T(\hat{n}') \Delta T(\hat{n}) \rangle$ is the underlying correlation function relevant for cosmology. It is evident from Eq.(27), that SI violation can occur either due rotational invariance breakdown of the true underlying temperature correlation function, $C(\hat{n}_1, \hat{n}_2) \not\equiv C(\hat{n}_1 \cdot \hat{n}_2)$, or, due to the breakdown of circularity in beam response function $B(\hat{n}_1, \hat{n}_2) \not\equiv B(\hat{n}_1 \cdot \hat{n}_2)$.

If the underlying CMB signal respects statistical isotropy (SI) symmetry as widely assumed in cosmology, then

$$C(\hat{n}_1, \hat{n}_2) = \sum_l \frac{2l+1}{4\pi} C_l \; W_l(\hat{n}_1, \hat{n}_2), \tag{28}$$

where $W_l(\hat{n}_1, \hat{n}_2)$ is the *elementary window function* [1] that accounts for effect of the finite resolution of beam function, given as

$$W_l(\hat{n}_1, \hat{n}_2) = \int d\Omega_{\hat{n}} \int d\Omega_{\hat{n}'} B(\hat{n}_1, \hat{n}) B(\hat{n}_2, \hat{n}') P_l(\hat{n} \cdot \hat{n}'). \tag{29}$$

Inverse transform of Eq.(4), yields the CMB BipoSH coefficients, $\tilde{A}^{LM}_{l_1 l_2}$ in terms of beam-BipoSH coefficients as

$$\tilde{A}^{LM}_{l_1 l_2} = \int d\Omega_{n_1} \int d\Omega_{n_2} \tilde{C}(\hat{n}_2, \hat{n}_2) \{ Y_{l_1}(\hat{n}_1) \otimes Y_{l_2}(\hat{n}_2) \}^*_{LM} \tag{30}$$

Hence, when the underlying CMB signal is statistically isotropic and beams are circular, BipoSH coefficient are expected to vanish for $L > 0$, refer Eq.(8),

$$\tilde{A}^{LM}_{l_1 l_2} = (-1)^{l_1} \prod_{l_1} C_{l_1} B^2_{l_1} \delta_{l_1 l_2} \delta_{L0} \delta_{M0}. \tag{31}$$

In Sec. III, we show that non-circularity of the beam response function is captured by beam-BipoSH coefficients. The BipoSH coefficients of CMB map for a reflection symmetric beam function can then be derived in terms of beam-BipoSH coefficients as (see Appendix A),

$$\tilde{A}^{LM}_{l_1 l_2} = \sum_l (-1)^l C_l \sum_{L_1 M_1 L_2 M_2} B^{L_1 M_1}_{l_1 l} B^{L_2 M_2}_{l_2 l} \prod_{L_1 L_2} C^{LM}_{L_1 M_1 L_2 M_2} \begin{Bmatrix} l & l_2 & L_2 \\ L & L_1 & l_1 \end{Bmatrix}. \tag{32}$$

In Sec. III, we also argued that it is convenient, as well as observationally motivated, to carry out the analytic analysis in a coordinate system where parallel-transport (PT) scan approximation holds and, consequently, the non-zero beam-BipoSH are restricted to $M = 0$. Eq. (32) then dictates that the corresponding BipoSH coefficients of the CMB maps are also restricted to $M = 0$ and are given by

$$\tilde{A}^{L0}_{l_1 l_2} = \sum_l (-1)^l C_l \sum_{L_1 L_2} B^{L_1 0}_{l_1 l} B^{L_2 0}_{l_2 l} \prod_{L_1 L_2} C^{L0}_{L_1 0 L_2 0} \begin{Bmatrix} l & l_1 & L_2 \\ L & L_1 & l_2 \end{Bmatrix}. \tag{33}$$

Since there is a triangularity condition ($|L_1 - L_2| \leq L \leq L_1 + L_2$), therefore the most dominant term in the above summation are $\{L_1 = L, L_2 = 0\}$ and $\{L_1 = 0, L_2 = L\}$.

The BipoSH estimator used by the WMAP team [24, 37], that differs from the original BipoSH definition in Hajian & Souradeep [28] by a factor of $\prod_L / (\prod_{l_1 l_2} C^{L0}_{l_1 0 l_2 0})$ are restricted to only even-parity BipoSH. *We insert this factor in the BipoSH expression in order to allow comparison to the published WMAP measurements more transparent* [47]

$$\tilde{A}^{L0}_{l_1 l_2} \rightarrow \frac{\prod_L}{\prod_{l_1 l_2} C^{L0}_{l_1 0 l_2 0}} \tilde{A}^{L0}_{l_1 l_2} \,. \tag{34}$$

SI violation signals in WMAP-7 were measured in two BipoSH spectra, A^{20}_{ll} and A^{20}_{l-2l}, we provide explicit leading order expressions for these coefficients arising from the NC-beam as,

$$\tilde{A}^{20}_{ll} = \frac{(-1)^l \, 2\sqrt{5} \, C_l \, B^{00}_{ll} B^{20}_{ll}}{(\prod_l)^3 C^{20}_{l0l0}} \,, \tag{35}$$

$$\tilde{A}^{20}_{l-2l} = \frac{\sqrt{5}(-1)^l}{\prod_{l-2l} C^{20}_{l-20l0}} \Big[\frac{C_{l-2} B^{00}_{l-2l-2} B^{20}_{ll-2}}{\prod_{l-2}} + \frac{C_l B^{00}_{ll} B^{20}_{l-2l}}{\prod_l} \Big] \,. \tag{36}$$

Note, that BipoSH expression in Eqs. (35) and (36) are provided in the scaled form that matches the BipoSH estimator employed by the WMAP team.

A. BipoSH from test Elliptical Gaussian beam model

Elliptic-Gaussian (EG) functions provide a simple model NC-beam extension to the oft-used circular-symmetric Gaussian beam function. The non-circularity is clearly parametrized by the eccentricity of the elliptical iso-contour lines. An EG-beam function pointed along $\hat{z}$ axis can be expressed in spherical polar coordinates, as

$$B(\hat{z}, \hat{n}) \;=\; \frac{1}{2\pi\sigma_1\sigma_2} \exp\left[-\frac{\theta^2}{2\sigma^2(\phi)} \right] , \tag{37}$$

where the azimuth angle dependent beam-width $\sigma(\phi_1) \;\equiv\; [\sigma_1^2/(1+\epsilon\sin^2\phi_1)]^{1/2}$ is given by Gaussian widths σ_1 and σ_2 along the semi-major and semi-minor axes. The non-circularity parameter $\epsilon \;=\; (\sigma_1^2/\sigma_2^2 - 1)$ is related to eccentricity $e = \sqrt{1-\sigma_2^2/\sigma_1^2}$ of the elliptical iso-contours. As expected, the Elliptical-Gaussian beam reduces to circular Gaussian beam for zero eccentricity ($e = 0$). Higher the value of eccentricity, stronger the deviation from circularity. An analytical expression for the beam-SH of EG-beam is available

$$b_{lm}(\hat{z}) \;=\; \begin{cases} \sqrt{\frac{(2l+1)(l+m)!}{4\pi(l-m)!}} (l+\frac{1}{2})^{-m} I_{m/2}\Big[(l+\frac{1}{2})^2 \frac{\sigma_1^2 e^2}{4} \Big] \exp\big[-(l+\frac{1}{2})^2 \frac{\sigma_1^2}{2}(1-\frac{e^2}{2}) \big] & (m \equiv \text{even}) \\ 0 & (m \equiv \text{odd}) \end{cases} \tag{38}$$

where $I_\nu(x)$ is the modified Bessel function [1]. The discrete even-fold azimuthal symmetry and reflection symmetry dictates $b_{lm} = 0$ for odd m. The reality condition of beam, $b^*_{lm} = b_{lm}$ for even m, then implies $b_{l-m} = b_{lm}$.

For Elliptical-Gaussian beams, the ratio b_{lm}/b_{l0} dies down rapidly with $|m|$. Hence, for mild eccentricities of the Elliptical beam, it is sufficient to consider only the lowest $m = 2$ mode. In Fig. 2, we plot spherical harmonic transform of an Elliptical-Gaussian beam with $\theta_{FWHM} = 13.579'$, which is close to θ_{FWHM} of W band of WMAP (with ellipticity $e = 0.4$ that best matches WMAP-7 W-band BipoSH spectra amplitude). Similarly, we also consider a EG-beam with $\theta_{FWHM} = 17.7036'$ close to the V-band beam. (The best fit to V-band BipoSH spectra corresponds ellipticity $e = 0.46$). For analysis purpose, it is a good enough approximation to restrict to $m = 0, \pm 2$ modes. We estimate beam-BipoSH coefficient in Eq.(25) for the case of "non-rotating" beams, $\rho = 0$ by using the closed analytical form of b_{lm}'s. Finally, using Eq.(35) and Eq.(36) we obtain the CMB BipoSH spectra A^{20}_{ll} and A^{20}_{l-2l} that were measured to be non-zero in WMAP-7. We verify the analytical results and compute the error bars on the BipoSH coefficients using statistically isotropic Gaussian simulations convolved with EG-beam functions. In Fig. 3, the analytic calculations of CMB-BipoSH for two cases of EG-beam are shown overlaid on estimates from average measurements with error-bars from 100 numerical simulations of noise free SI maps convolved with corresponding NC-beams. The results with test elliptical-Gaussian beams serve to crosscheck and validate our analytical expression derived and a check the numerical simulation of CMB maps convolved (in real space) with an NC-beam.

It is clear that NC-beams generate detectable levels of non-zero CMB BipoSH. The CMB-BipoSH spectra A^{20}_{ll} and A^{20}_{l-2l} are both proportional to the the leading order non-circular correction, $b_{l0} b_{l2}$ and the underlying SI CMB

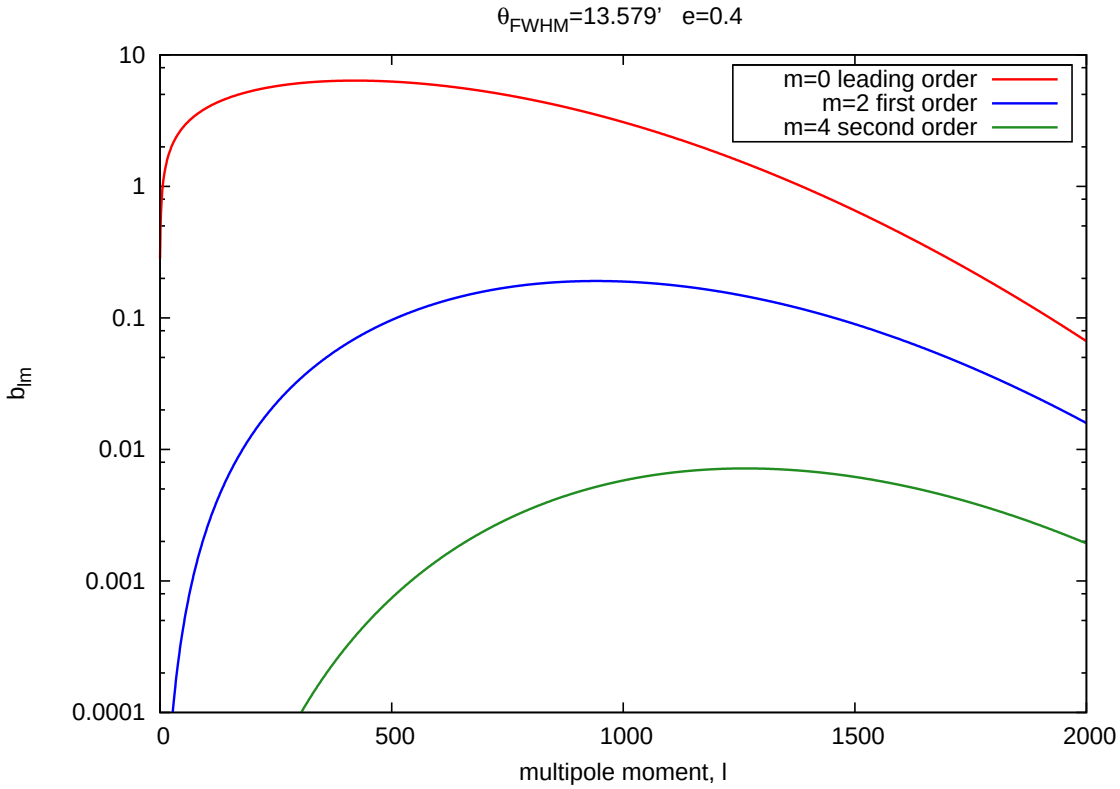

FIG. 2: Harmonic transforms of an elliptical Gaussian beam with $\theta_{FWHM} = 13.579'$ and ellipticity $e = 0.4$. The circular symmetric component of the NC EG-beam is given by is $m = 0$ and $m = 2$ captures the leading order EG-beam effect.

power spectrum (see Eqs. (33) and (24)). It is instructive to compare the EG-model beam predictions to the WMAP BipoSH measurements. Using Elliptical-Gaussian beams with FWHM values close to the WMAP W and V band reproduces detectable peak structure in the BipoSH spectra. The amplitudes can be matched by choosing appropriate values of effective eccentricity for the V ($e = 0.46$) and W bands ($e = 0.4$). Although, the eccentricity of the WMAP beams can be estimated for raw beam maps [2], it is expected that multiple visits by the beam at any pixel with varying orientation in WMAP scan would tend to reduce the effective eccentricity to smaller values. The eccentricities that reproduce the correct amplitudes for the CMB-BipoSH roughly correspond to the reduction also indicated from comparing the corrections to the angular power spectrum [40]). The fact that both the A^{20}_{ll} and A^{20}_{l-2l} spectra, are roughly matched in amplitude and qualitative peak structure with the correct relative sign, for identical ellipticity parameters, then suggests that the WMAP-7 BipoSH measurements may have actually captured subtle uncorrected NC-beam effects.

V. BIPOSH SIGNATURES OF NON-CIRCULARITY IN WMAP BEAMS

While CMB BipoSH from the test elliptical-Gaussian NC-beam motivates a more careful estimation of the NC-beam effect in WMAP-7 maps, these fail to reproduce a key qualitative feature of WMAP BipoSH measurements; viz. the change in sign of the V-band A^{20}_{ll} at large multipoles. This, however, is not surprising. It is widely-known that the WMAP beams deviate from a Gaussian profile and that an Elliptical Gaussian beam is not a good approximation [2, 41, 42]. In section V A, we first use the SH transform of the raw WMAP beam maps to compute the CMB-BipoSH under PT-scan approximation. Interestingly, we recover qualitative features in BipoSH spectra measurements that were not captured by the Elliptical Gaussian beams. As expected the amplitude of the CMB-BipoSH based raw beam are much higher in amplitude relative to the measurements. A rudimentary numerical superposition of raw beam transforms to mimic the effect of multiple hits with varying orientation at a pixel (using a WMAP scan), leads us to expect a constant scaling of the leading order b_{l2} by a factor $\alpha \sim 0.4$. More a detailed analytics treatment presented in the Appendix C that allows for deviations from PT-scan approximation in averaging

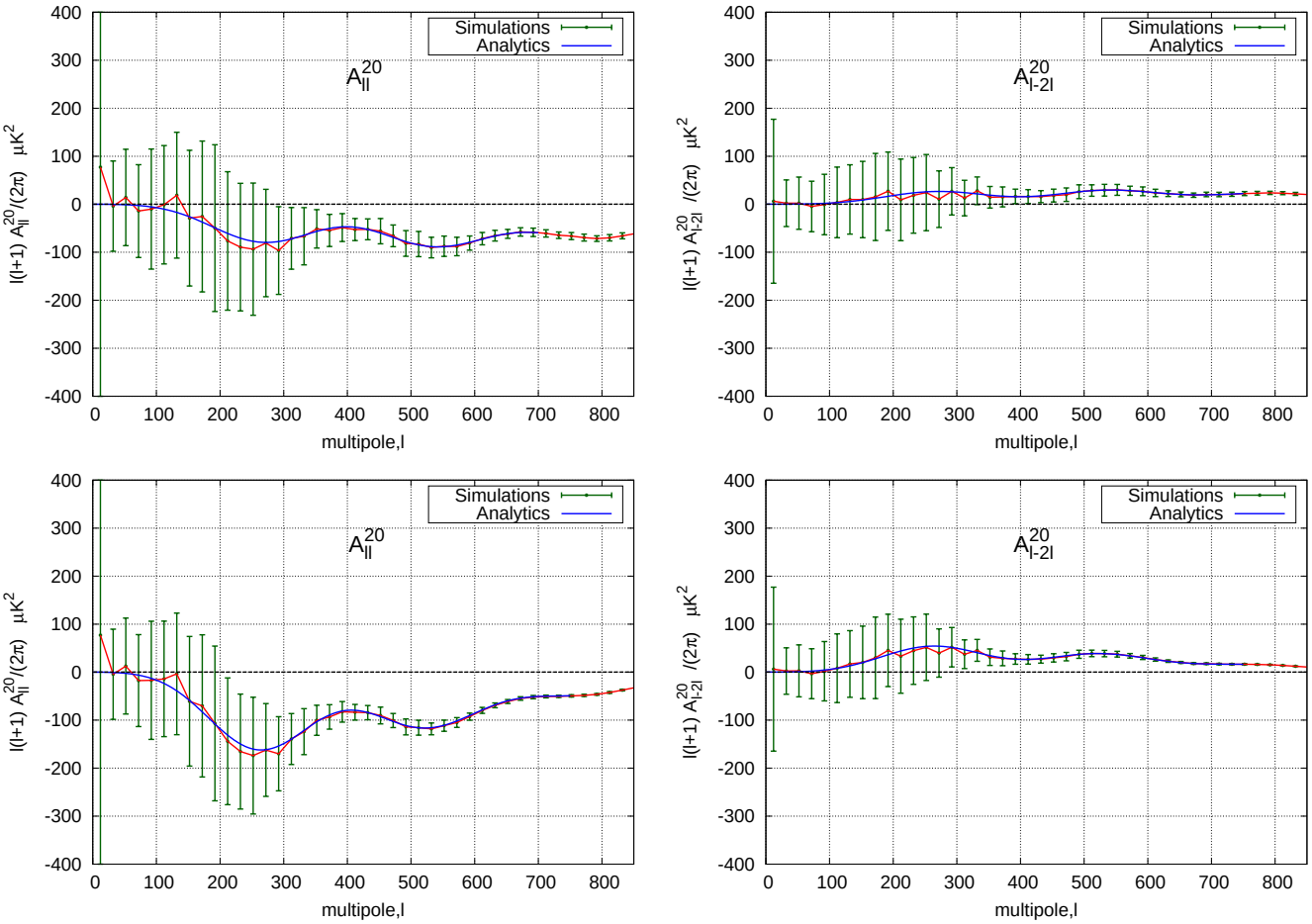

FIG. 3: BipoSH spectra A^{20}_{ll} and A^{20}_{l-2l} for an elliptical Gaussian beam with : (*Top*) $\theta_{FWHM} = 13.579'$ and ellipticity $e = 0.4$; (*Bottom*) $\theta_{FWHM} = 17.7036'$ and ellipticity $e = 0.46$ smooth (blue) curve are binned CMB-BipoSH computed using the analytic expressions. The red curve with corresponding error-bars are obtained from 100 numerical simulated SI maps convolved with the same elliptical Gaussian beam. The underlying SI signal corresponds to the best fit Λ-CDM model from WMAP7

over multiple hits, reveals multipole l dependent correction, f_l to the constant scaling that depends on the detailed scan strategy of the CMB experiment over all multiple hits.

The analytic expression for f_l in Appendix C, for simplicity, pertains only to a single beam scan case. In particular, the approach cannot account for any complexities that may be introduced to the effective NC-beam that is used estimates the BipoSH spectra arising due to linear algebraic map-making procedure from two beam differencing. However, it motivates the exploration of phenomenological effective beam $b^{\rm eff}_{lm} = \sum_{m'} F_{lm'} b_{lm'}$ expressed in terms of the beam-SH obtained from the raw beam maps. We proceed with the assumption that the WMAP BipoSH measurements arise from NC-beam effect and take the 'phenomenological' approach to determine b_{l2} from BipoSH measurements. Limiting attention to the leading order contribution at $m = 2$ we parametrize the function $f_l \equiv F_{l2}$ and fit to the measured BipoSH spectra. In section V B, we first fit for a constant value α that most closely reproduces the WMAP BipoSH measurements. While we find that $\alpha \sim 0.4$ is the best-fit value, the goodness of fit is not very satisfactory. We find that a linear correction to the constant scaling, $b^{\rm eff}_{l2} = (\alpha + \beta \cdot l) b_{l2}$ provides very good fits to the WMAP BipoSH measurements. Numerical simulations incorporating complexities of two beam differencing and map-making procedure and deviations from PT-scan approximation are needed to decide whether the parameters of the phenomenological scaling obtained are justified.

A. BipoSH coefficients from single-side WMAP raw beam map

To mimic NC-beams closer to WMAP, we consider the A side raw beam maps of the V2 and W1 differencing Assembly (DA) of WMAP as representative of the V and W band beams, respectively. We compute the beam-SH coefficients for these numerically for use in semi-analytic estimate of the CMB BipoSH coefficients,using Eqs. (35) and (35). Fig. 4 gives plots of the circular, b_{l0} and leading order b_{l2} beam-SH coefficients of the W1A and V2A raw beam maps. Note that the b_{l2} spectrum changes sign and takes negative values at large l – a key qualitative feature of the WMAP beams that cannot be captured in Elliptical-Gaussian models where b_{l2} does not change sign with l. The origin of this curious feature becomes apparent in the raw beam maps of the W1A and V2A channel shown in Fig. 5. The central part of the beam maps show an elliptical peak with marked non-trivial non-circular 'shoulder-like' features. However, more interesting are the right-hand panels, where we highlight a spread out annular distribution of regions with negative response. The integrated power in the negative beam response ~ 0.5 of the total power and has significant impact on the beam-SH. In particular, it leads to negative values of b_{l2} at $l \gtrsim 2\sigma_b^{-1}$. We find that this feature is critical in recovering the qualitative feature in V-band A_{ll}^{20} changing sign at large l seen in the WMAP measurements. Since such an unique correspondence between a beam-SH feature and the consequent CMB BipoSH is unlikely to be mimicked by other effects. We claim that this provides a strong hint that WMAP BipoSH measurements are linked to the NC-beam effect.

We use PT-scan approximation in ecliptic coordinates given the fact that the WMAP BipoSH results indicate azimuthal symmetry of SI violation ($M = 0$) in ecliptic coordinates. The analytical results are verified using numerical simulations of the BipoSH coefficients A_{ll}^{20} and A_{l-2l}^{20} are shown in Fig. 6. As seen in Fig. 6, the amplitudes of the BipoSH coefficients do not match with WMAP7 year's observed detections. This is expected as the BipoSH coefficients are obtained from the A side beam of a single channel in W and V band without accounting for circularizing of the beam due to multiple hits with varying orientations. We collate and list some key similarity of these results to the detections of SI violation in WMAP-7 data:

1. As expected from analytic understanding, the numerical simulations also confirm that the most significant contribution is the $M = 0$ mode in BipoSH spectra A_{ll}^{2M} and A_{l-2l}^{2M} when the analysis is done in ecliptic coordinates, giving strength to our PT-scan approximation. In a coordinate system where PT-scan approximation is valid only $M = 0$ mode should be significant.

2. We notice the NC beam effect is larger in W band than in V band explaining the difference in detected SI violation signal at the two frequencies.

3. We recover the change of sign of the BipoSH A_{ll}^{20} measurements at large l in the V-band.

4. The BipoSH coefficients from NC beam shows a prominent bump roughly around the first acoustic peak ($l = 220$) for both W and V band. This corresponds mainly to the scale picked by the underlying angular power spectrum C_l. However, the precise peak location also depends on the peak in $b_{l0}b_{l2}$ for each band and can account for differences in the peak location in the two bands shown in Figure 4.

The exercise of computing BipoSH from single side raw beam maps under PT-scan approximation does provide motivation for a deeper analysis of the NC-beam effect in the WMAP-7 maps. Numerically simulated maps incorporating the two side WMAP beam differencing, scan and map-making details should settle the extent to which approximations used here are valid and clearly settle the question of whether the entire WMAP-7 BipoSH signal arises as an effect of uncorrected NC-beam effects. Implementing numerical simulation with actual WMAP beam maps present serious computational challenge. Besides the main central peak having significant structure, the WMAP beams have a spread-out annular pattern of negative response that cannot be neglected. This implies that for a careful BipoSH analysis of SI violation, a convolution with much larger regions of the WMAP beam maps of W and V band, extending roughly to, $\sim 10\theta_{FWHM}$, is required making it computationally expensive. The beam maps of W1A and V2A channel are shown in Fig.5. In particular, we highlight the spread-out negative part of the beam response that explains some unique qualitative features of the WMAP BipoSH measurements.The power in the negative part of the beam is more than 50 percent of its central positive peak and hence, non negligible. Work is in progress and results will be presented in the near future.

B. Fitting BipoSH spectra measurements to an effective NC-beam

In the analytic approach we show that the BipoSH coefficients scales as $A_{l_1 l_2}^{20} \propto b_{l_1 0} b_{l_2 2}$ for mild deviations from circular beams under PT-scan as given in Eq. (33). However, realistically, complex details of relative orientation of A

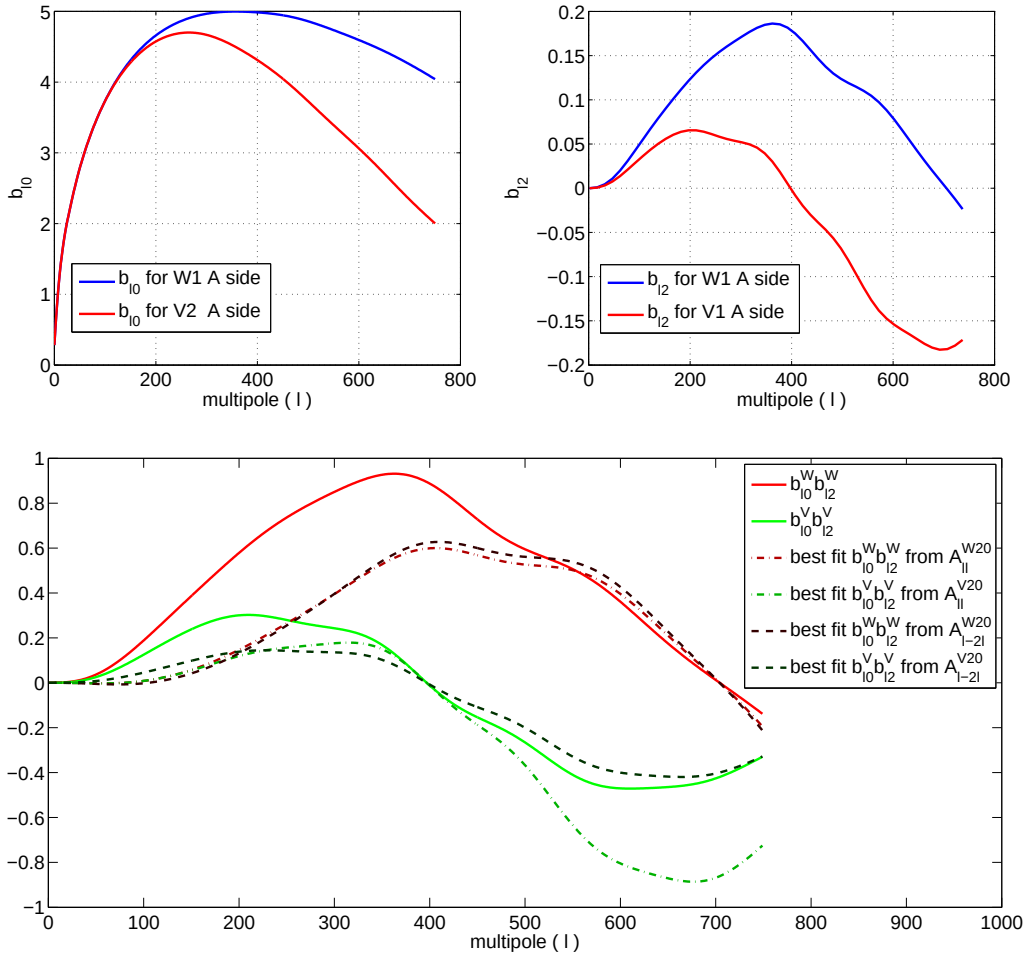

FIG. 4: *Top:* Beam spherical harmonic transforms, b_{l0} and b_{l2} of beam maps of A side of W1 and V2 DA. It is interesting to note that $|b_{l2}|/b_{l0} \lesssim 0.01$ implying the BipoSH representation is sensitive to really really subtle levels of non-circularity in the beams.

Bottom: The plot of the NC-beam leading order NC beam perturbation parameter $b_{l0}b_{l2}$ vs. l . The solid lines correspond to beam-SH of the raw beam maps, the dashed lines show the $b_{l0}b_{l2}^{\rm eff}$ of the phenomenological best-fit effective beam-SH $b_{l2}^{\rm eff} = f_l b_{l2}$ obtained by parametrized linear fits to f_l using the the two measured BipoSH spectra, A_{ll}^{20} and A_{l-2l}^{20} The plots also show that although BipoSH peak structure is largely set by the underlying angular power spectrum C_l of SI cosmological mode, small differences observed at the two different frequencies can arise because of the difference in the shapes of $b_{l0}b_{l2}$.

and B side of beams for each DA, the differencing scheme and map-making, the varying orientations for the multiple hits at each pixel in the actual scan strategy, etc., all could have bearing at finer levels on CMB BipoSH generated by the NC-beam.

As shown in Appendix C, the averaging of the NC-beam at any pixel due to multiple-hits at different orientations can be expected to lead to simply a scaling of $b_{l2}^{\rm eff} = f_l b_{l2}$. This would correspondingly scale BipoSH spectra obtained from A side beam of W1 and V2 channel by f_l.

Retaining PT scan approximation, the superposition of raw beam transforms leads us to expect a constant scaling $f_l = \alpha$. The value $\alpha \sim 0.4$ most closely reproduces the WMAP BipoSH spectra. We confirm this to be consistent with numerical estimates from beam-SH superposition using $\rho_i(\hat{n})$ obtained from WMAP-like multiple hits but with PT-scan approximation (see Appendix C. The numerical value of α depends on the unknown relative orientations of the A and B side beams (assumed to be identical) and matches the fit value of α for relative orientation $\sim 140°$.

However, the goodness of fit for constant f_l is not very satisfactory in explaining the entire WMAP-7 BipoSH spectra in terms of NC-beam systematics and suggests that l-dependence of f_l may be important for a finer match. While, in principle, it is possible to determine f_l for the WMAP scan by numerical superposition of beam-SH using

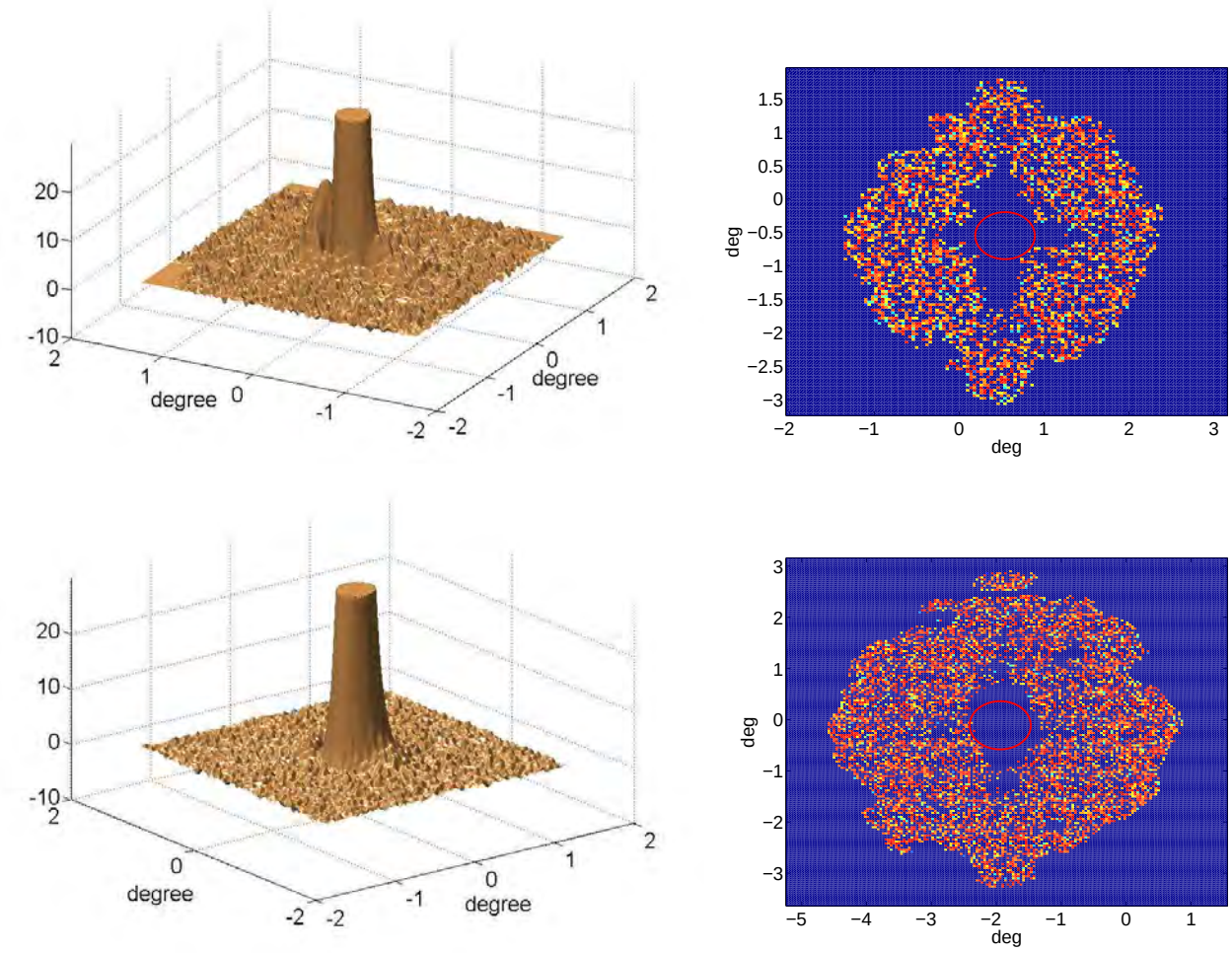

FIG. 5: Beam response function of A side of W1 differencing assembly *(Top)* and A side of V2 differencing assembly *(Bottom)* are shown. The *Left-hand* panels show 3D zoomed view of the central part of the beam shows a truncated view of the central beam peak to clearly highlight the elliptical contour. Marked non-circular shoulder features are seen in the central peak. The *Right-hand* panels cover the entire beam-map images to show the spread-out annular distribution of regions with negative response. (The red circles marks the central beam peak region). The power in negative response is ~ 0.5 of the positive power in the central peaks. The annular negative power distribution shows quadrupolar feature that modifies the beam-SH b_{l2} to take negative values at high l for the V-band (see Fig 6). The corresponding impact of this beam-SH is significant and crucial for understanding the intriguing qualitative zero-crossing feature in the V-band BipoSH spectra. It is apparent then that correctly accounting for WMAP NC-beam effects numerically in our ongoing analysis, requires the convolution of almost the entire beam map region with the SI sky-map leading to enormous increase in computing costs (relative to using only the central peak).

Eq. (C11). Practically, it will be plagued by ambiguity of relative orientation of the A and B side NC-beams and many other finer details. Hence, we prefer to take a phenomenological approach and explore parametrized f_l that fit the BipoSH measurements. *Minimally, this provides an effective beam that would explain the observed WMAP-7 BipoSH spectra under PT-scan approximation. We believe that this provides a computationally inexpensive approach to quantify the WMAP NC-beam systematic effect.*

The obvious step beyond constant scaling, would be to add a linear correction $f_l = \alpha 1 + \beta * l$. As shown in Fig. 7) we find very good fits to the WMAP BipoSH measurements with this scaling. Interestingly enough, it seems possible to find values of α and β that simultaneously provide fairly good fits to both A^{20}_{ll} and A^{20}_{l-2l} BipoSH spectra. Note that the product $b_{l0}b_{l2}$ still tends to zero for large l as seen in the bottom panel of Fig. 4.

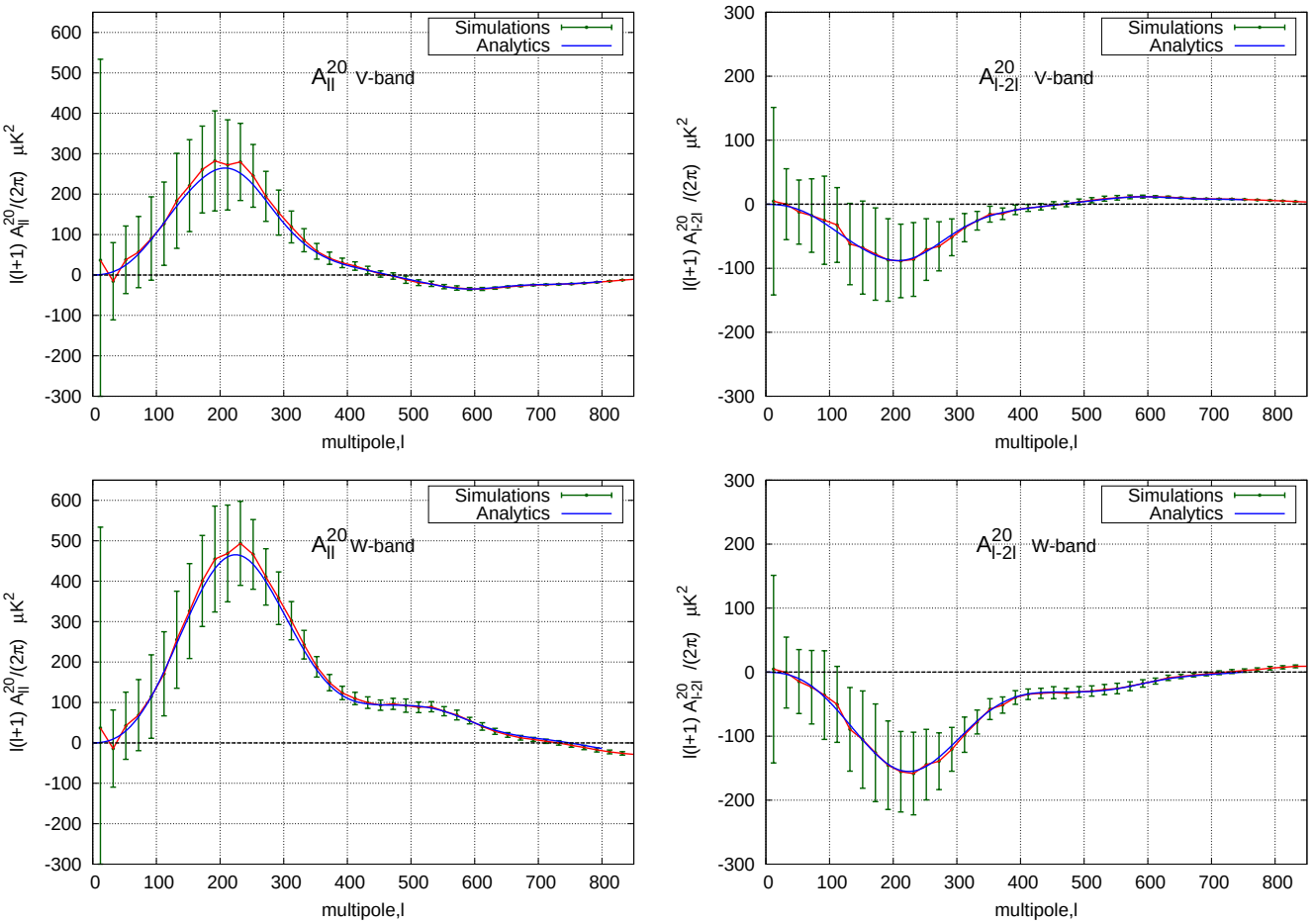

FIG. 6: BipoSH spectra, A^{20}_{ll} (*Left*) and A^{20}_{l-2l} (*Right*) obtained for the raw beam maps A side of V2 channel (*Top*) and A side of W1 channel (*Bottom*) of the WMAP experiment. Analytically evaluated BipoSH spectra (blue) overlaid on the average BipoSH spectra (red) with error bars obtained from 100 simulations of statistically isotropic CMB sky convolved W1 and V2 channel of WMAP. While the BipoSH spectra from raw beam-SH recover interesting qualitative features of the measure spectra, the amplitudes need to be corrected for the circularizing effect of averaging raw beam maps with multiple hits with varying orientation at any pixel.

VI. DISCUSSIONS & CONCLUSION

The observed CMB sky is a convolution of the cosmological signal with the instrumental beam response function of the experiment (assuming perfect removal of foreground emissions, etc.). The deconvolution of the beam effect from the signal is relatively straightforward for an ideal circular symmetric beam. Non-Circular (NC) deviations of the beam , however mild, are practically inevitable in all experiments, and affect the results obtained at the limits of the sensitivity and resolution of the recent experiments. The effect of WMAP NC-beam on the angular power spectrum C_l is not very pronounced and is significant only at very large multipoles. It is, hence, very interesting that CMB maps obtained with NC-beams disrupt the rotational invariance of the two point correlation function of the cosmological CMB signal, theoretically expected from the 'cosmological principle', leading to clearly measurable signatures of Statistical Isotropy (SI) violation.

We show that SI violation measures in the Bipolar Spherical Harmonic (BipoSH) representation of the observed CMB maps, are well-suited to capture systematic NC-beam effect. It is important to note that even though the level of non circularity is WMAP beams is at $\sim 1\%$ percent, the BipoSH spectra generated by this effect are measurable. This points to immense promise and potential of the BipoSH representation also as a diagnostic tool for current and future CMB experiments. A key objective is also to assess whether the recent measurement of non-zero BipoSH spectra, A^{20}_{ll} and A^{20}_{l-2l} in WMAP-7 in the V & W band maps [24] could arise from uncorrected NC-beam effects in WMAP-7 maps.

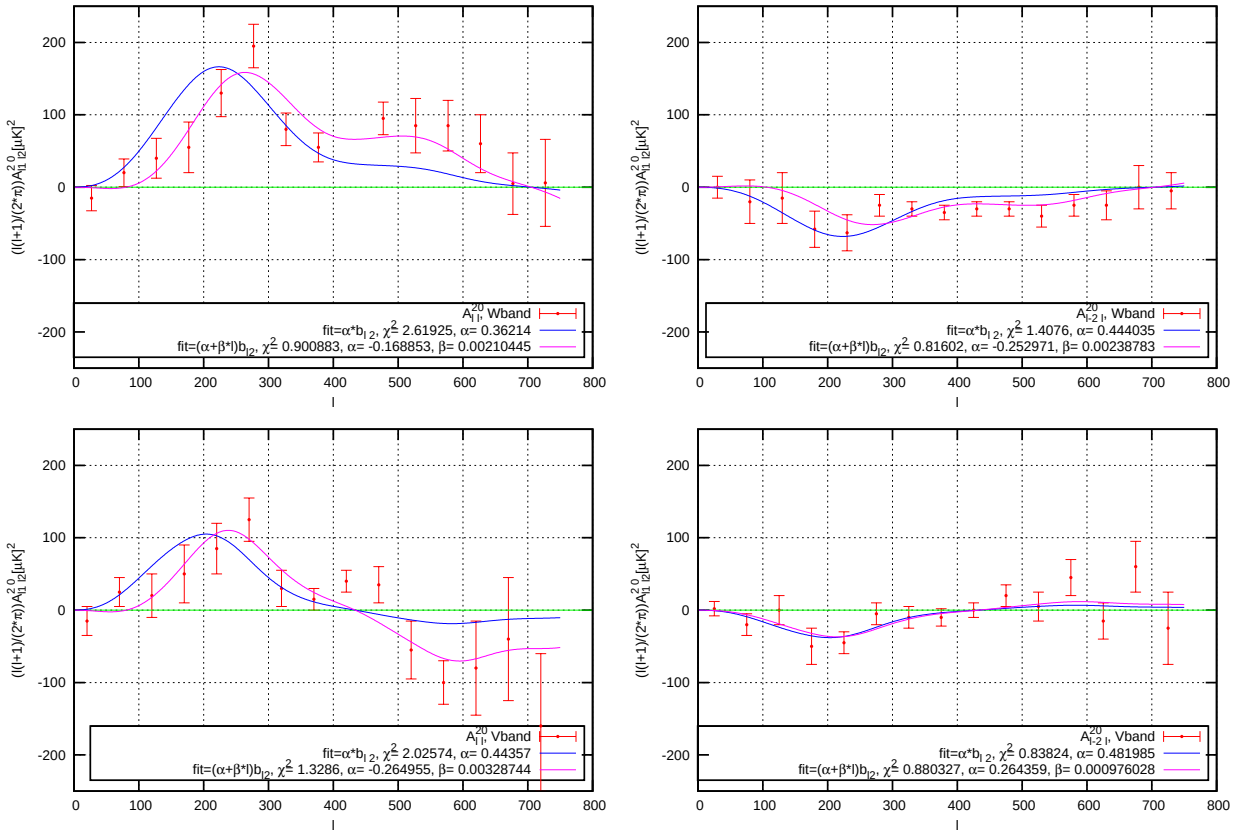

FIG. 7: Comparison of BipoSH spectra generated by effective NC-beams at the V and W bands to the published WMAP-7 BipoSH spectra measurements (approximately digitized from the Fig 16 of Ref. [24]). As described in Appendix C, an effective NC-beam can be constructed from from the raw beam-SH, b_{lm} given by $b^{\rm eff}_{lm} = \sum_{m'} F_{lm'} b_{lm'}$. The measured BipoSH spectra, A^{20}_{ll} and A^{20}_{l-2l}, are sourced at the leading order by the $m = 2$ term. Hence we estimate the parametrized fits to the function $f_l \equiv F_{l2}$ using the W and V band BipoSH measurements. We present the best fit results for a constant $f_l = \alpha$ and a linear function $f_l = (\alpha + \beta \cdot l)$. The respective values of the reduced χ^2 of the fit and the best-fit parameters are provided in the figure. The constant, f_l, provides a fit that partially accounts for the BipoSH spectra detections in terms of WMAP NC-beam effect. However, remarkably an effective $b^{\rm eff}_{l2}$ from the linear form of f_l can satisfactorily explain the non-zero BipoSH spectra detected in WMAP-7 in terms of the corresponding V and W band effective NC-beams.

In this paper, we introduce the novel and useful concept of expanding the NC-beam response function in the BipoSH basis to define beam-BipoSH coefficients. The beam-BipoSH not only incorporate the effect of the NC-beam (expressed in terms of the beam-SH – the spherical harmonic transform of the beam $b_{lm}(\hat{z})$ pointing at $\hat{z}$), but also the additional effect of the scan strategy that determines the beam orientation angle, $\rho(\hat{n})$ relative to the local longitude at any pixel. Neat and completely analytic results for CMB BipoSH generated by NC-beams can be obtained within the 'parallel-transport' (PT) scan approximation where the beam visits the pixels at constant $\rho(\hat{n}) \equiv \rho$. We argue that this approximation is observationally well-motivated due to the azimuthal symmetry ($M = 0$) in the WMAP-7 BipoSH measurements in the ecliptic coordinates. All analytical results are verified using corresponding numerical simulations on SI maps convolved with NC-beam in the PT-approximation. The numerical simulations also provide estimates of the error-bars, hence, a measure of the significance of carious features in the predicted BipoSH spectra.

As a test case we first work with Elliptical-Gaussian beam with adjustable eccentricity but FWHM that match the V and W band WMAP beams. Elliptical-Gaussian beams have clearly interpreted NC parameters and also permits a well-controlled perturbation treatment for non-circular deviations (b_{lm}/b_{l0} dies rapidly with $|m|$ [1]). This exercise also provides a reliable test case to cross-check analytic results with that obtained from numerical simulations of SI maps convolved with NC-beams. At the leading order ($b_{l2}b_{l0}$), we recover significant CMB BipoSH coefficients A^{20}_{ll} and A^{20}_{l-2l} with broadly correct qualitative features – relative sign difference in the two spectra and a well understood peak structure defined by the acoustic features in underlying C_l modulated by spectral shape of $b_{l0}b_{l2}$. We choose

the eccentricity parameters at fixed FWHM to match the amplitude. We conclude that the multiple visits of the beam reduces the eccentricity by a factor comparable to that indicated by comparing non-circular beam corrections to WMAP C_l from semi-analytic and numerical estimates [2, 40, 42].

As may be expected, the Elliptical-Gaussian approximation to WMAP beams, completely fails to recover certain qualitative features of the BipoSH measurements, in particular, the change of sign in the V-band A^{20}_{ll} at large l. This is addressed next by computing the beam-SH for single (A) side WMAP beam maps for V and W bands. The beam maps show a marked annular region well beyond a few FWHM from the center where the beam response is negative. This leads to the b_{l2} going negative at large multipoles beyond the beam-width and explains the change in sign of V-band BipoSH at larger l. Note that Elliptical-Gaussian can never recover this feature, since $b_{l2} \geq 0$. Again, as expected, the amplitude of the CMB-BipoSH based on beam-SH, b_{l2}, from raw beam maps are much higher. An analytic treatment of superposition of raw beam transforms to mimic the effect of multiple hits with varying orientation at a pixel, leads us to expect a scaling of the leading order term $b^{\rm eff}_{l2} = f_l b_{l2}$. However, f_l depends on the detailed and accurate scan description of each beam and many other finer details of the instruments. Hence we choose to adopt a 'phenomenological' approach to determine the effective beam by fitting parametrized f_l to the WMAP-7 BipoSH spectra measurements assuming it to be entirely sourced by NC-beam effect. A constant $f_l = \alpha \approx 0.4$ provides only a fair fit and does not account for the entire signal. A linear correction to the constant scaling, $f_l = \alpha + l\dot{\beta}$ allows for very good fits to the WMAP BipoSH spectra measurements as shown in Fig. 7.

Complexities of two beam differencing and map-making procedure, deviations from PT-scan approximation, etc., may account for the phenomenologically obtained f_l scaling of raw beam-SH, b_{l2}. If confirmed in our ongoing numerical simulations with realistic WMAP scan and full beam map convolution, we can firmly conclude that NC-beam effects are completely responsible for the WMAP-7 BipoSH measurements. In any case, our results indicate clearly that a major portion of the BipoSH signal measured in WMAP-7 may be attributed to an experiment specific systematic effect arising from uncorrected NC-Beam effect. However, it is still possible that the BipoSH measurements are not entirely explained by the NC beam effect leaving room for an achromatic component from intrinsic cosmological SI violation. Since the WMAP-7 BipoSH signal are strong and significant, other full sky CMB experiments with comparable, or better, sensitivity and angular resolution should readily confirm, or disprove this possibility. In near future, good quality full sky CMB polarization maps when available can also be studied in the BipoSH representation [32] and will provide an independent window in to SI violation phenomena.

Acknowledgments

We simulate CMB maps with the HEALPix [43] package additional modules added for real-space convolution with NC-beams. Computations were carried out at the HPC facilities at IUCAA. NJ, SD and AR acknowledge the Council of Scientific and Industrial Research (CSIR), India for financial support through Senior Research fellowships. NJ thanks IUCAA for hosting visits to facilitate the collaborative effort. NJ also acknowledges useful discussions and encouragement from Sanjay Jhingan at her home institution. SM acknowledges support from his DST fast-track grant. TS acknowledges support from the Swarnajayanti fellowship grant, DST, India.

Appendix A: Beam BipoSH

Beam-BipoSH are expansion coefficients of the beam response function in BipoSH basis (see Sec III). The most general beam-BipoSH in any coordinate system is given by,

$$B^{LM}_{l_1 l_2} = \sum_{m_1 m_2} C^{LM}_{l_1 m_1 l_2 m_2} \sum_{m'} b_{l_2 m'}(\hat{z}) \int_{\theta=0}^{\pi} \int_{\phi=0}^{2\pi} D^{l_2}_{m_2 m'}(\phi, \theta, \rho(\theta,\phi)) Y^*_{l_1 m_1}(\theta,\phi) \sin\theta d\theta d\phi. \tag{A1}$$

Wigner-D functions can be expressed in terms of Wigner-d through following relation,

$$D^l_{mm'}(\phi,\theta,\rho) = \mathrm{e}^{-im\phi}\, d^l_{mm'}(\theta)\, \mathrm{e}^{-im'\rho}\,, \tag{A2}$$

and reduces to spherical harmonics for $m' = 0$,

$$D^l_{m0}(\phi,\theta,\rho) = \sqrt{4\pi/(2l+1)} Y^*_{lm}(\theta,\phi)\,. \tag{A3}$$

In the parallel-transport (PT) scan approximation, the beam orientation, with respect to the local Cartesian

coordinate aligned with the spherical (θ,ϕ) coordinates, does not vary on sky (i.e., $\rho(\theta,\phi)\equiv\rho$), the beam-BipoSH

$$B^{LM}_{l_1l_2} = \sqrt{\frac{2l_1+1}{4\pi}}\sum_{m'} b_{l_2m'}\exp^{-im'\rho}\sum_{m_1m_2} C^{LM}_{l_1m_1l_2m_2}\int_{\phi=0}^{2\pi}\exp^{-i(m_1+m_2)\phi}\,d\phi\int_{\theta=0}^{\pi} d^{l_2}_{m_2m'}(\theta)d^{l_1}_{m_10}(\theta)d(\cos\theta) \quad \text{(A4)}$$

$$= 2\pi\delta_{M0}\sum_{m'} b_{l_2m'}(\hat{z})\exp^{-im'\rho}\sum_{m_2}(-1)^{m_2}C^{L0}_{l_1-m_2l_2m_2}I^{l_1l_2}_{m_2,m'} \quad \text{(A5)}$$

is derived to be non-zero only for $M=0$, using the orthogonality relation,

$$\int_{\phi=0}^{2\pi}\exp^{-i(m_1+m_2)\phi}\,d\phi = 2\pi\delta_{m_1,-m_2}. \quad \text{(A6)}$$

We define the notation

$$I^{l_1l_2}_{m_2,m'} = (-1)^{m_2}\sqrt{\frac{(2l_1+1)}{4\pi}}\int_{\theta=0}^{\pi} d^{l_2}_{m_2m'}(\theta)d^{l_1}_{m_20}(\theta)d(\cos\theta). \quad \text{(A7)}$$

Here we have used $d^l_{mm'}(\theta)=(-1)^{m-m'}d^l_{-m-m'}(\theta)$. To simplify the analytic expressions, we retain only the leading order NC beam spherical harmonic mode $m'=2$, assuming mild NC-beam with discrete even-fold azimuthal symmetry where no odd m' modes will contribute. Hence, the summation over m' has three terms corresponding to $m'=0,\pm2$.

The beam-BipoSH can be then be written as

$$B^{LM}_{l_1l_2} \equiv B^{LM^{(C)}}_{l_1l_2} + B^{LM^{(NC)}}_{l_1l_2} \quad \text{(A8)}$$

$$B^{LM^{(C)}}_{l_1l_2} = 2\pi\,\delta_{L0}\,\delta_{M0}\;b_{l_20}(\hat{z})\sum_{m_2} C^{L0}_{l_1-m_2l_2m_2}I^{l_1l_2}_{m_2,0}$$

$$B^{LM^{(NC)}}_{l_1l_2} = 2\pi\delta_{M0}\sum_{m_2\neq0} C^{L0}_{l_1-m_2l_2m_2}\Big(b_{l_2-2}(\hat{z})\exp^{i2\rho}\,I^{l_1l_2}_{m_2,-2} + b_{l_22}(\hat{z})\exp^{-i2\rho}\,I^{l_1l_2}_{m_2,2}\Big). \quad \text{(A9)}$$

First term in Eq.(A8) is the trivial beam-BipoSH, $B^{00^{(C)}}_{ll}$, corresponding to the circular symmetric component of the beam response function. Non circular part of the beam function $m'=\pm2$, gives rise to beam BipoSH having $L\neq0$. First, we evaluate the beam-BipoSH due to circular part of beam function. Orthogonality of Wigner-d functions,

$$\int_0^{\pi} d(\cos\theta)\,d^l_{mm'}(\theta)d^{l'}_{mm'}(\theta) = \frac{2}{2l+1}\delta_{ll'} \quad \text{(A10)}$$

implies

$$I^{l_1l_2}_{m_2,0} = (-1)^{m_2}\Big(\frac{2}{2l_2+1}\Big)\sqrt{\frac{(2l_1+1)}{4\pi}}\delta_{l_1l_2}. \quad \text{(A11)}$$

Using the following property of Clebsch-Gordan ,

$$\sum_m(-1)^{l-m}C^{L0}_{lml-m} = \sqrt{(2l+1)}\delta_{L0}. \quad \text{(A12)}$$

we obtain

$$B^{LM(C)}_{l_1l_2} = \sqrt{4\pi}(-1)^{l_2}b_{l_20}(\hat{z})\delta_{l_1l_2}\delta_{L0}\delta_{M0}. \quad \text{(A13)}$$

Since,

$$b_{l0}(\hat{z}) = \sqrt{\frac{(2l+1)}{4\pi}}B_l, \quad \text{(A14)}$$

where B_l is the usual beam transfer function of the circular-symmetrized beam profile,

$$B^{LM(C)}_{l_1l_2} = (-1)^{l_2}\sqrt{2l_2+1}B_{l_2}\delta_{l_1l_2}\delta_{L0}\delta_{M0}. \quad \text{(A15)}$$

Next, we analytically calculate the beam-BipoSH $B^{LM^{(NC)}}$ due to the non circular part of the beam function,

$$B^{LM^{(NC)}}_{l_1 l_2} = 2\pi\sqrt{\frac{(2l_1+1)}{4\pi}}\delta_{M0}\sum_{m_2}(-1)^{m_2}C^{L0}_{l_1-m_2 l_2 m_2}\Big[\, b_{l_2-2}(\hat{z})\exp^{i2\rho}\int_{\theta=0}^{\pi} d^{l_2}_{m_2-2}(\theta)d^{l_1}_{m_2 0}(\theta)d(\cos\theta) + b_{l_2 2}(\hat{z})\exp^{-i2\rho}\int_{\theta=0}^{\pi} d^{l_2}_{m_2 2}(\theta)d^{l_1}_{m_2 0}(\theta)d(\cos\theta)\Big]. \tag{A16}$$

In the above expression, the summation is over m_2. It is convenient to separate the calculation of the $m_2 = 0$ and rest of the $m_2 \neq 0$ terms.

Consider the integral for $m_2 = 0$. For this we use, $d^l_{mm'} = (-1)^{m+m'}d^l_{m'm}$ and expansion of Wigner-d's in terms of associated Legendre polynomials, $d^l_{m0}(\theta) = (-1)^m\sqrt{(l-m)!/(l+m)!}P^m_l(\cos\theta)$, and obtain

$$\int_{\theta=0}^{\pi} d^{l_2}_{02}(\theta)d^{l_1}_{00}(\theta)d(\cos\theta) = \sqrt{\frac{(l_2-2)!}{(l_2+2)!}}\int_{\theta=0}^{\pi} P^2_{l_2}(\cos\theta)P_{l_1}(\cos\theta)d(\cos\theta)\,. \tag{A17}$$

Using standard recurrence relations of Associated Legendre functions,

$$P^2_l(\cos\theta) = \frac{2\cos\theta}{\sin\theta}P^1_l(\cos\theta) - l(l+1)P_l(\cos\theta), \tag{A18}$$

$$P^1_l(\cos\theta) = \sin\theta P'_l(\cos\theta), \tag{A19}$$

and orthogonality relations,

$$\int_{\theta=0}^{\pi} P_{l_2}(\cos\theta)P_{l_1}(\cos\theta)d(\cos\theta) = \frac{2}{2l_2+1}\delta_{l_1 l_2}\,, \tag{A20}$$

$$\int_{\theta=0}^{\pi}\cos\theta P'_{l_2}(\cos\theta)P^0_{l_1}(\cos\theta)d(\cos\theta) = \begin{cases} 0 & \text{if } (l_1+l_2 = \text{odd}) \\ 0 & \text{if } (l_1 > l_2) \\ 0 & \text{if } (l_1 < l_2) \\ \frac{2l_2}{2l_2+1} & \text{if } (l_1 = l_2)\,. \end{cases} \tag{A21}$$

Therefore, for $m_2 = 0$, the integral simplifies to

$$I^{l_1 l_2}_{0,\pm 2} = (-1)^{m_2}\sqrt{\frac{(2l_1+1)}{4\pi}}\begin{cases} 0 & \text{if } (l_1+l_2 = \text{odd}) \\ 0 & \text{if } (l_1 > l_2) \\ 4\sqrt{\frac{(l_2-2)!}{(l_2+2)!}} & \text{if } (l_1 < l_2) \\ \sqrt{\frac{(l_2-2)!}{(l_2+2)!}}\big[\frac{4l_2}{(2l_2+1)} - \frac{2l_2(l_2+1)}{(2l_2+1)}\big] & \text{if } (l_1 = l_2)\,. \end{cases} \tag{A22}$$

Next, we consider the $m_2 \neq 0$ terms in the summation in Eq.(A16). Here, $d^{l_2}_{m_2 2}(\theta)$ can be recursively reduced to $d^{l_2}_{m_2 0}(\theta)$ using the following recurrence relation,

$$d^{l_2}_{m_2 2}(\theta) = \frac{\kappa}{\sin^2\theta}\Big[\kappa_0 d^{l_2}_{m_2 0}(\theta) + \kappa_1 d^{l_2+1}_{m_2 0}(\theta) + \kappa_{-1}d^{l_2-1}_{m_2 0}(\theta) + \kappa_2 d^{l_2+2}_{m_2 0}(\theta) + \kappa_{-2}d^{l_2-2}_{m_2 0}(\theta)\Big] \tag{A23}$$

where,

$$\kappa_0 \equiv \frac{m_2^2}{l_2^2(l_2+1)^2} - \frac{l_2^2-m_2^2}{l_2^2(4l_2^2-1)} - \frac{(l_2+1)^2-m_2^2}{(l_2+1)^2(2l_2+1)(2l_2+3)},$$

$$\kappa_1 \equiv 2m_2\frac{\sqrt{(l_2+1)^2-m_2^2}}{l_2(l_2+1)(l_2+2)(2l_2+1)},\quad \kappa_{-1} \equiv -2m_2\frac{\sqrt{l_2^2-m_2^2}}{l_2(l_2^2-1)(2l_2+1)},$$

$$\kappa_2 \equiv \frac{\sqrt{[(l_2+1)^2-m_2^2][(l_2+2)^2-m_2^2]}}{(l_2+1)(l_2+2)(2l_2+1)(2l_2+3)} \text{ and } \kappa_{-2} \equiv \frac{\sqrt{(l_2^2-m_2^2)[(l_2-1)^2-m_2^2]}}{l_2(l_2-1)(4l_2^2-1)}\,.$$

Under reflection Wigner-d's, $d^l_{mm'}(\pi-\theta)=(-1)^{l+m'}d^l_{m-m'}(\theta)$.

$$d^{l_2}_{m_2-2}(\theta)=\frac{\kappa}{\sin^2\theta}\left[\kappa_0 d^{l_2}_{m_20}(\theta)-\kappa_1 d^{l_2+1}_{m_20}(\theta)-\kappa_{-1}d^{l_2-1}_{m_20}(\theta)+\kappa_2 d^{l_2+2}_{m_20}(\theta)+\kappa_{-2}d^{l_2-2}_{m_20}(\theta)\right] \tag{A24}$$

and then as shown in [2], the integrals for $m_2\neq 0$ terms are obtained as

$$I^{l_1l_2}_{m_2,\pm 2} = (-1)^{m_2}\sqrt{\frac{(2l_1+1)}{4\pi}}\begin{cases}\Big(\frac{\kappa\kappa_0}{|m_2|}+\frac{\kappa\kappa_2}{|m_2|}\sqrt{\frac{(l_2+|m_2|)!(l_2+2-|m_2|)!}{(l_2-|m_2|)!(l_2+2+|m_2|)!}} & \\ +\frac{\kappa\kappa_{-2}}{|m_2|}\sqrt{\frac{(l_2-|m_2|)!(l_2-2+|m_2|)!}{(l_2+|m_2|)!(l_1-2-|m_2|)!}}\Big) & \text{if } (l_1=l_2)\\ \Big(\frac{\kappa\kappa_0}{|m_2|}\sqrt{\frac{(l_2+|m_2|)!(l_1-|m_2|)!}{(l_2-|m_2|)!(l_1+|m_2|)!}}+\frac{\kappa\kappa_2}{|m_2|}\sqrt{\frac{(l_2+2+|m_2|)!(l_1-|m_2|)!}{(l_2+2-|m_2|)!(l_1+|m_2|)!}}+ & \\ \frac{\kappa\kappa_{-2}}{|m_2|}\sqrt{\frac{(l_2-2+|m_2|)!(l_1-|m_2|)!}{(l_2-2-|m_2|)!(l_1+|m_2|)!}}\pm\frac{\kappa\kappa_1}{|m_2|}\sqrt{\frac{(l_2+1+|m_2|)!(l_1-|m_2|)!}{(l_2+1-|m_2|)!(l_1+|m_2|)!}} & \\ \pm\frac{\kappa\kappa_{-1}}{|m_2|}\sqrt{\frac{(l_2-1+|m_2|)!(l_1-|m_2|)!}{(l_2-1-|m_2|)!(l_1+|m_2|)!}}\Big) & \text{if } (l_1>l_2)\\ \Big(\frac{\kappa\kappa_0}{|m_2|}\sqrt{\frac{(l_1+|m_2|)!(l_2-|m_2|)!}{(l_1-|m_2|)!(l_2+|m_2|)!}}+\frac{\kappa\kappa_2}{|m_2|}\sqrt{\frac{(l_2+2-|m_2|)!(l_1+|m_2|)!}{(l_2+2+|m_2|)!(l_1-|m_2|)!}} & \\ +\frac{\kappa\kappa_{-2}}{|m_2|}\sqrt{\frac{(l_2-2-|m_2|)!(l_1+|m_2|)!}{(l_2-2+|m_2|)!(l_1-|m_2|)!}}\pm\frac{\kappa\kappa_1}{|m_2|}\sqrt{\frac{(l_2+1-|m_2|)!(l_1+|m_2|)!}{(l_2+1+|m_2|)!(l_1-|m_2|)!}} & \\ \pm\frac{\kappa\kappa_{-1}}{|m_2|}\sqrt{\frac{(l_2-1-|m_2|)!(l_1+|m_2|)!}{(l_2-1+|m_2|)!(l_1-|m_2|)!}}\Big) & \text{if } (l_1<l_2)\,.\end{cases}$$

In general, NC-beams would generate both even-parity and odd-parity beam-BipoSH coefficients

$$B^{LM^{(NC)}}_{l_1l_2}=B^{LM^{(+)}}_{l_1l_2}+B^{LM^{(-)}}_{l_1l_2}\,. \tag{A25}$$

The even-parity beam-BipoSH,

$$B^{LM^{(+)}}_{l_1l_2} = \begin{cases}\delta_{M0}[b_{l_22}(\hat z)\exp(-i2\rho)+b^*_{l_22}(\hat z)\exp(i2\rho)](-C^{L0}_{l_10l_20}\sqrt{\frac{4\pi l_2(l_2-1)}{(2l_2+1)(l_2+2)(l_2+1)}}+ & \\ 2\pi\sqrt{\frac{(2l_1+1)}{4\pi}}\sum_{|m_2|>0}C^{L0}_{l_1-m_2l_2m_2}\big[\frac{\kappa\kappa_0}{|m_2|}+\frac{\kappa\kappa_2}{|m_2|}\sqrt{\frac{(l_2+|m_2|)!(l_2+2-|m_2|)!}{(l_2-|m_2|)!(l_2+2+|m_2|)!}} & \\ +\frac{\kappa\kappa_{-2}}{|m_2|}\sqrt{\frac{(l_2-|m_2|)!(l_2-2+|m_2|)!}{(l_2+|m_2|)!(l_1-2-|m_2|)!}}\big]) & \text{if } (l_1=l_2 \text{ and } l_2\geq 2)\\ \delta_{M0}[b_{l_22}(\hat z)\exp(-i2\rho)+b^*_{l_22}(\hat z)\exp(i2\rho)]2\pi\sqrt{\frac{(2l_1+1)}{4\pi}}(\sum_{|m_2|>0}C^{L0}_{l_1-m_2l_1m_2}\times & \\ \big[\frac{\kappa\kappa_0}{|m_2|}\sqrt{\frac{(l_2+|m_2|)!(l_1-|m_2|)!}{(l_2-|m_2|)!(l_1+|m_2|)!}}+\frac{\kappa\kappa_2}{|m_2|}\sqrt{\frac{(l_2+2+|m_2|)!(l_1-|m_2|)!}{(l_2+2-|m_2|)!(l_1+|m_2|)!}}+ & \\ \frac{\kappa\kappa_{-2}}{|m_2|}\sqrt{\frac{(l_2-2+|m_2|)!(l_1-|m_2|)!}{(l_2-2-|m_2|)!(l_1+|m_2|)!}}\big]) & \text{if } (l_1>l_2 \text{ and } l_2\geq 2)\\ \delta_{M0}[b_{l_22}(\hat z)\exp(-i2\rho)+b^*_{l_22}(\hat z)\exp(i2\rho)](8\pi C^{L0}_{l_10l_20}\sqrt{\frac{(2l_1+1)(l_2-2)!}{4\pi(l_2+2)!}}+ & \\ 2\pi\sqrt{\frac{(2l_1+1)}{4\pi}}\sum_{|m_2|>0}C^{L0}_{l_1-m_2l_1m_2}\big[\frac{\kappa\kappa_0}{|m_2|}\sqrt{\frac{(l_1+|m_2|)!(l_2-|m_2|)!}{(l_1-|m_2|)!(l_2+|m_2|)!}}+ & \\ \frac{\kappa\kappa_2}{|m_2|}\sqrt{\frac{(l_2+2-|m_2|)!(l_1+|m_2|)!}{(l_2+2+|m_2|)!(l_1-|m_2|)!}}+\frac{\kappa\kappa_{-2}}{|m_2|}\sqrt{\frac{(l_2-2-|m_2|)!(l_1+|m_2|)!}{(l_2-2+|m_2|)!(l_1-|m_2|)!}}\big]) & \text{if } (l_1<l_2 \text{ and } l_2\geq 2)\,,\end{cases}$$

and odd parity-beam-BipoSH,

$$B^{LM^{(-)}}_{l_1 l_2} = \begin{cases} 0 & \text{if } (l_1 = l_2) \\ \delta_{M0}[b_{l_2 2}(\hat{z})\exp(-i2\rho) - b^*_{l_2 2}(\hat{z})\exp(i2\rho)]2\pi\sqrt{\frac{(2l_1+1)}{4\pi}}(\sum_{|m_2|>0} C^{L0}_{l_1 -m_2 l_1 m_2}\times \\ \left[\frac{\kappa\kappa_1}{|m_2|}\sqrt{\frac{(l_2+1+|m_2|)!(l_1-|m_2|)!}{(l_2+1-|m_2|)!(l_1+|m_2|)!}} + \frac{\kappa\kappa_{-1}}{|m_2|}\sqrt{\frac{(l_2-1+|m_2|)!(l_1-|m_2|)!}{(l_2-1-|m_2|)!(l_1+|m_2|)!}}\right]) & \text{if } (l_1 > l_2 \text{ and } l_2 \geq 2) \\ \delta_{M0}[b_{l_2 2}(\hat{z})\exp(-i2\rho) - b^*_{l_2 2}(\hat{z})\exp(i2\rho)]2\pi\sqrt{\frac{(2l_1+1)}{4\pi}}(\sum_{|m_2|>0} C^{L0}_{l_1 -m_2 l_1 m_2}\times \\ \left[\frac{\kappa\kappa_1}{|m_2|}\sqrt{\frac{(l_2+1-|m_2|)!(l_1+|m_2|)!}{(l_2+1+|m_2|)!(l_1-|m_2|)!}} + \frac{\kappa\kappa_{-1}}{|m_2|}\sqrt{\frac{(l_2-1-|m_2|)!(l_1+|m_2|)!}{(l_2-1+|m_2|)!(l_1-|m_2|)!}}\right]) & \text{if } (l_1 < l_2 \text{ and } l_2 \geq 2) \end{cases}$$

To avoid any confusion, we reiterate that the above results hold for PT-scan approximation and a NC-beam function with discrete even-fold azimuthal symmetry. Other residual symmetries in NC-beam can reduce the set of non-zero beam BipoSH further. In particular, if the experimental beam has reflection symmetry, then odd parity beam BipoSH will vanish and only even parity ones will be present. This implies that odd parity beam BipoSH can be used as a measure of breakdown of reflection symmetry in NC-beams.

Appendix B: CMB BipoSH due to Non-circular beam effect

The cosmological signal in the observed temperature fluctuations is convolved with instrumental beam response function. So even if the underlying cosmological temperature fluctuations are statistically isotropic, non circularity of the beam can give rise to detections in BipoSH coefficients. In this appendix we provide a detailed derivation of the BipoSH coefficient arising from non circular beam presented in Sec. IV. The measured temperature fluctuation map $\widetilde{\Delta T}(\hat{n}_1)$ is a convolution

$$\widetilde{\Delta T}(\hat{n}_1) = \int d\Omega_{n_2} B(\hat{n}_1, \hat{n}_2)\Delta T(\hat{n}_2). \tag{B1}$$

of the cosmological signal $\Delta T(\hat{n}_2)$ with the beam response function $B(\hat{n}_1, \hat{n}_2)$ that encodes the sensitivity of the instrument around the pointing direction, $\hat{n}_1$ and can be expanded in the spherical harmonic (SH) basis,

$$\Delta\tilde{T}(\hat{n}) = \sum_{lm} \tilde{a}_{lm} Y_{lm}(\hat{n}). \tag{B2}$$

Similarly, the cosmological signal decomposed in the SH basis, as

$$\Delta T(\hat{n}) = \sum_{lm} a_{lm} Y_{lm}(\hat{n})\,. \tag{B3}$$

Beam response function can be expanded in the BipoSH basis,

$$B(\hat{n}_1, \hat{n}_2) = \sum_{l_1 l_2 LM} B^{LM}_{l_1 l_2} \sum_{m_1 m_2} Y_{l_1 m_1}(\hat{n}_1) Y_{l_1 m_1}(\hat{n}_2). \tag{B4}$$

Using orthogonality of spherical harmonics,

$$\int d\Omega_{\hat{n}} Y_{lm}(\hat{n}) Y_{l'm'}(\hat{n}) = (-1)^{m'}\delta_{ll'}\delta_{mm'}\,, \tag{B5}$$

we obtain

$$\widetilde{\Delta T}(\hat{n}_1) = \sum_{l_1 m_2} \sum_{lmLM} (-1)^m a_{lm} B^{LM}_{l_1 l} C^{LM}_{l_1 m_1 l -m} Y_{l_1 m_1}(\hat{n}_1). \tag{B6}$$

Using the above expansion together with Eq.(B2), we obtain,

$$\tilde{a}_{l_1 m_1} = \sum_{lmLM} (-1)^m a_{lm} B^{LM}_{l_1 l} C^{LM}_{l_1 m_1 l -m}. \tag{B7}$$

and the harmonic space covariance as

$$\langle \tilde{a}_{l_1 m_1} \tilde{a}_{l_2 m_2} \rangle = \sum_{lmLM} \sum_{l'm'L'M'} (-1)^{m+m'} \langle a_{lm} a_{l'm'} \rangle B^{LM}_{l_1 l} B^{LM}_{l_2 l'} C^{LM}_{l_1 m_1 l -m} C^{L'M'}_{l_2 m_2 l' -m'} \,. \tag{B8}$$

Assuming the cosmological signal to be statistically isotropic,

$$\langle a_{lm} a_{l'm'} \rangle = (-1)^m C_l \delta_{ll'} \delta_{m-m'}. \tag{B9}$$

and substituting in Eq.(B8), we obtain the SH-space covariance of the observed map as

$$\langle \tilde{a}_{l_1 m_1} \tilde{a}_{l_2 m_2} \rangle = \sum_{lmLM} \sum_{L'M'} (-1)^m C_l B^{LM}_{l_1 l} B^{L'M'}_{l_2 l} C^{LM}_{l_1 m_1 l -m} C^{L'M'}_{l_2 m_2 lm} \tag{B10}$$

As given in Eq.(6), CMB BipoSH coefficients are related to the SH space covariance matrix in Eq. (B8), leading to

$$\tilde{A}^{L_1 M_1}_{l_1 l_2} = \sum_{lLL'MM'} C_l B^{LM}_{l_1 l} B^{L'M'}_{l_2 l} \sum_{mm_1 m_2} (-1)^m C^{LM}_{l_1 m_1 l -m} C^{L'M'}_{l_2 m_2 lm} C^{L_1 M_1}_{l_1 m_1 l_2 m_2} \tag{B11}$$

The sum over product of three Clebsch-Gordan coefficients can be written compactly in terms of a 6-j symbol, as

$$\sum_{\alpha\beta\delta} (-1)^{a-\alpha} C^{c\gamma}_{a\alpha b\beta} C^{e\epsilon}_{d\delta b\beta} C^{f\varphi}_{d\delta a-\alpha} = K_1 \prod_{cf} C^{e\epsilon}_{c\gamma f\varphi} \begin{Bmatrix} a & b & c \\ e & f & d \end{Bmatrix}, \tag{B12}$$

where $K_1 = (-1)^{b+c+d+f}$ and $\prod_{cf} = \sqrt{(2c+1)(2f+1)}$. In a PT-scan approximation, $M = 0, M' = 0, M_1 = 0$. Hence, we obtain the expression in Eq. (32) for CMB BipoSH coefficient from NC-beam with PT-scan approximation

$$\tilde{A}^{L_1 M_1}_{l_1 l_2} = \delta_{M_1 0} \sum_{lLL'} C_l B^{L0}_{l_1 l} B^{L'0}_{l_2 l} (-1)^{l_1 + L' - L_1} \sqrt{(2L+1)(2L'+1)} C^{L_1 0}_{L0L'0} \begin{Bmatrix} l & l_1 & L \\ L_1 & L' & l_2 \end{Bmatrix}. \tag{B13}$$

The Clebsch-Gordan coefficient $C^{L_1 0}_{L0L'0}$ is zero when the sum $L + L' + L_1$ is odd valued, hence, enforces the condition that the summation in the above expression is limited to $L + L' + L_1$ being even-valued. When the beam function has an even fold azimuthal symmtery and reflection symmetry beam-BipoSH coefficients are restricted to even parity and follows $l_1 + l_2 =$ even, then L and L' are restricted to even multipole values. Thereafter, due to the presence of $C^{L_1 0}_{L0L'0}$, L_1 takes up even multipole values.

Appendix C: Effective beam averaged over multiple hits with varying orientations

We present an analytic treatment to cover NC-beam effect incorporating the multiple hits at any pixel $\hat{n}$ by the NC-beam with fixed shape but at varying orientations, $\rho_j(\hat{n})$. This information can be obtained from the instrument design description and the scan-strategy of the experiment over the duration of the data acquisition.

The observed temperature anisotropy for a single hit by the beam at a direction $\hat{n} \equiv (\theta, \phi)$ with orientation, $\rho_j(\hat{n})$ is given by

$$\widetilde{\Delta T}(\hat{n}) = \int d\Omega_{n'} B(\hat{n}, \hat{n}'; \rho_i(\hat{n}))\ \Delta T(\hat{n}') \,, \tag{C1}$$

where $\Delta T(\hat{n}')$ is the cosmological signal. Simply generalizing the notations for Eqs. (9) to (11) in Sec. III, we write

$$B(\hat{n}, \hat{n}'; \rho_i(\hat{n})) = \sum_{lm} b_{lm}(\hat{n}; \rho_i)\, Y_{lm}(\hat{n}') \tag{C2}$$

$$= \sum_{lm} \left[\sum_{m'} b_{lm'}(\hat{z}) D^l_{mm'}(\phi, \theta, \rho_i(\hat{n})) \right] Y_{lm}(\hat{n}') \tag{C3}$$

$$= \sum_{lm} \left[\sum_{m'} b_{lm'}(\hat{z})\, d^l_{mm'}(\theta)\, \mathrm{e}^{-im\rho_j(\hat{n})} \right] \mathrm{e}^{-im\phi}\, Y_{lm}(\hat{n}') \,. \tag{C4}$$

where we relate the beam function in terms of beam-SH, $b_{lm'}(\hat{z})$ as done in Eq. (11).

Next, we define an effective beam-SH $b^{\rm eff}_{lm'}(\hat{z})$ averaged over $N(\hat{n})$ multiple hits at pixel, $\hat{n}$, and over the whole sky

$$b^{\rm eff}_{lm}(\hat{z}) \equiv \int d\Omega_n \sum_{j=1}^{N(\hat{n})} \frac{1}{N(\hat{n})} b_{lm}(\hat{z};\rho_j(\hat{n})) = \sum_{m'} F_{lm'}\, b_{lm'}(\hat{z}) \tag{C5}$$

where it is easy to show that

$$F_{lm} = \sum_{m'} \int d\Omega_n\, d^l_{mm'}(\theta)\, {\rm e}^{-im\phi} \frac{1}{N(\hat{n})} \sum_{j=1}^{N(\hat{n})} {\rm e}^{-im'\rho_j(\hat{n})}\,. \tag{C6}$$

The above provides the general expression for the beam-SH of the effective beam for a single beam experiment given the beam-SH from the raw beam map and entire scan pattern history, $\rho_j(\hat{n})$. Note, it is tedious, but conceptually straightforward, to extend this formalism to account for two beam differencing even with different A and B side NC-beam by separating the averages over $b^{A,B}_{lm'}(\hat{z};\rho^{(A,B)}_j(\hat{n})$ with appropriate signs and weights. However, the limitation of this approach is that it does not capture the effect of the linear algebraic step of map-making carried out to covert difference measurements between different pixels into temperature fluctuations map.

In this paper, we have evaluated analytic expressions only up to to the leading order effect at $m = 2$. Since the WMAP beams seem mildly NC-beams where $|b_{lm}|/b_{l0}$ become smaller with larger $|m|$ (at least for lowest few values of $m > 2$ that were explicitly checked). Hence, we provide explicit expressions for $b^{\rm eff}_{l2}$ from Eq (C6), limiting to beam-SH $b_{lm}(\hat{z}) = b_{l0}\delta_{m0} + b_{l1}\delta_{m1} + b_{l2}\delta_{m2}$ (i.e., assuming mildly NC-beam) as

$$b^{\rm eff}_{l2}(\hat{z}) = b_{l0}(\hat{z})F_{l0} + b_{l1}(\hat{z})F_{l1} + b_{l2}(\hat{z})F_{l2} \tag{C7}$$

$$F_{l0} = \int d\Omega_n {\rm e}^{i\,2\phi} d^l 20 = \int d\Omega_n Y_{20}(\hat{n}) = b_{00}\delta_{l0} \tag{C8}$$

$$F_{l1} = \int d\Omega_n {\rm e}^{-i2\phi} \sum_{i=1}^{N(\hat{n})} \left[d^l_{2\,-1}(\theta){\rm e}^{i\rho(\hat{n})} + d^l_{21}(\theta){\rm e}^{-i\rho(\hat{n})}\right] \tag{C9}$$

$$F_{l2} = \int d\Omega_n {\rm e}^{-i2\phi} \sum_{i=1}^{N(\hat{n})} \left[d^l_{2\,-2}(\theta){\rm e}^{i2\rho(\hat{n})} + d^l_{22}(\theta){\rm e}^{-i2\rho(\hat{n})}\right]\,. \tag{C10}$$

The first term integrates to zero for $l > 0$. In our analytic expressions, we ignored, $b_{l1}(\hat{n})$,since it drops out in the PT-scan approximation even without reflection symmetry assumption. This may not necessarily be non-negligible here due to deviations from PT-scan approximation but we ignore it for simplicity. We finally obtain the scaling used in Sec. V B

$$b^{\rm eff}_{l2}(\hat{z}) = F_{l2} b_{l2}(\hat{z})$$

$$f_l \equiv F_{l2} = \int d\Omega_{\hat{n}} {\rm e}^{-i2\phi} \sum_{i=1}^{N(\hat{n})} \left[d^l_{2\,-2}(\theta)\, {\rm e}^{i2\rho(\hat{n})} + d^l_{22}(\theta)\, {\rm e}^{-i2\rho(\hat{n})}\right]\,. \tag{C11}$$

Invoking the approximation that $\rho_j(\hat{n}) \approx \rho_j$ is constant for each pass of the beam on the sky and equal number of visits, $f_l = \alpha$, can shown to be a constant, $|\alpha| < 1$. We use a simple model of the WMAP scan strategy [44] that provides an estimate of $\alpha \sim 0.4$ for identical A & B side beams at a relative angle of $\sim 140^\circ$ consistent with the best-fit α obtained from the BipoSH spectra. The simple WMAP scan model ignores, flagged portions of the actual time-line data, finer details of the location of the different frequency feed-horns from the spin-axis on the focal plane, etc., that may, or may not, be important. In the absence of unambiguous means to determine f_l, we resort to making a polynomial (in l) fit to f_l and find that a linear term is sufficient to provide good fits to the WMAP-7 BipoSH spectra measurements. From the analytic expression in Eq. (C11), apprpriate non-polynomial parametrized forms of f_l may yet be found to be better motivated.

[1] T. Souradeep, B. Ratra, ApJ **560**, 28-40, (2001).
[2] S. Mitra, A. S. Sengupta, T. Souradeep, Phys. Rev. D **70**, 103002 (2004).

[3] T. Souradeep, S. Mitra, A. S. Sengupta, S. Ray, R. Saha, New Astron. Rev. **50**, 2006.
[4] P. Fosalba, O. Doré, F. R. Bouchet, Phys. Rev. D **65**, 063003 (2002).
[5] S. Mitra et al, ApJS **193**, 5, (2011).
[6] B. D. Wandelt, K. M. Gorski, Phys. Rev. D **63**, 123002 (2001).
[7] G. Hinshaw et al., Astrophys. J. Suppl. **170**, 288 (2007).
[8] M. A. J. Ashdown et al., Astron. Astrophys. **467**, 761-775 (2007).
[9] M. Tegmark, A. de Oliveira-Costa and A. Hamilton, Phys. Rev. D **68**, 123523 (2003).
[10] P. Bielewicz, K. M. Gorski and A. J. Banday, Mon. Not. Roy. Astron. Soc. **355**, (2004).
[11] C. J. Copi, D. Huterer, D. J. Schwarz and G. D. Starkman, Mon. Not. Roy. Astron. Soc. **367**, (2006).
[12] K. Land and J. Magueijo, Phys. Rev. Lett. **95**, 071301 (2003).
[13] H. K. Eriksen, F. K. Hansen, A. J. Banday, K. M. Gorski and P.B. Lilje, Astrophys. J. **605**, 14 (2001).
[14] N. J. Cornish, D. N. Spergel and G. D. Starkman, Classical Quantum Gravity, **15**, 2657, (1998).
[15] J. Levin, Phys. Rept. **365**, (2002).
[16] M. Lachieze-Rey and J. P. Luminet, Phys. Rep. **25**, 136, (1995).
[17] M. Aich and T. Souradeep, Phys. Rev. D **81**, 083008 (2010).
[18] A. R. Pullen and M. Kamionkowski, Phys. Rev. D **76**, 103529 (2007).
[19] L. Ackerman and S. M. Carroll and M. B. Wise, Phys. Rev. D **75**, 083502 (2007).
[20] Aditya Rotti, Moumita Aich and Tarun Souradeep, arXiv:1111.3357v1 (2011).
[21] A.E. Gumrukcuoglu, Carlo R. Contaldi, M. Peloso, JCAP **11**, 005, (2007).
[22] J.R. Bond, D. Pogosyan and T. Souradeep, Phys.Rev. D62 (2000) 043006.
[23] T. Souradeep, Indian J. Phys. **80**, 1063-1069 (2006).
[24] C. L. Bennett et. al., Astrophys. J. Supplement Series **192**, 19 (2011).
[25] D. Hanson, A. Lewis and A. Challinor, Phys. Rev. D **81**, 103003 (2010).
[26] I. K. Wehus, L. Ackerman, H. K. Eriksen and N. E. Groeneboom, ApJ **707**, 343-353 (2009).
[27] Legacy Archive for Microwave Background Analysis http://lambda.gsfc.nasa.gov/.
[28] A. Hajian and T. Souradeep, Astrophys. J. Lett. **597**, L5 (2003).
[29] T. Souradeep and A. Hajian, Pramana **62**, 793-796 (2004).
[30] A. Hajian and T. Souradeep, arXiv:astro-ph/0501001 (2004).
[31] A. Hajian, T. Souradeep and N. Cornish, ApJ **618**, L63-L66 (2004).
[32] S. Basak, A. Hajian and T. Souradeep, Phys. Rev. D **74**, 021301 (2006).
[33] A. Hajian and T. Souradeep, Phys. Rev. D **74**, 123521 (2006).
[34] D. A. Varshalovich, A. N. Moskalev and V. K. Khersonskii, *Quantum Theory of Angular Momentum* (Singapore: World Scientific, 1988).
[35] N. Joshi, S. Jhingan, T. Souradeep, A. Hajian, Phys. Rev. D **81**, 083012 (2010).
[36] L. G. Book, M. Kamionkowski, T. Souradeep, Phys. Rev. D **85**, 023010 (2012).
[37] D. Hanson and A. Lewis, Phys. Rev. D **80**, 063004 (2009).
[38] A. Hajian, Doctoral thesis, IUCAA (Univ. of Pune), 2008.
[39] M. Kamionkowski and T. Souradeep, Phys. Rev. D **83**, 027301 (2011).
[40] S. Mitra, A. S. Sengupta, S. Ray, R. Saha, T. Souradeep, Mon. Not. Roy. Astron. Soc. **394**, (2009).
[41] L. Page et al.[WMAP collab. 1-year] Astrophys. J. Suppl. 148:39 (2003).
[42] G. Hinshaw et al. [WMAP collab. 3-year], Astrophys. J. Suppl. 170:288, (2007).
[43] K.M. Gorski et al., ApJ **622**, 759 (2005).
[44] Santanu Das and Tarun Souradeep, Proc. of ICGC-2011, *preprint* arXiv:1210.0004.
[45] Odd parity BipoSH coefficients are a measure of the breakdown of reflection symmetry in instrumental beams. Expressions for the odd parity BipoSH coefficients generated in absence of reflection-symmetry of the beam are provided in the appendix for completeness.
[46] Departure from reflection symmetry in the beam of a full-sky CMB experiment, if ignored, also causes leakage of power from the ~ 500 times stronger CMB dipole signal into higher multipole, most importantly, contaminating the CMB quadrupole moment of the angular power spectrum. This has been studied and estimates on WMAP beam maps indicates the effect of reflection breakdown symmetry is expected to be small, but not negligible [44].
[47] Note that this factor in WMAP-BipoSH estimator strictly restricts BipoSH considerations to the even parity sector since $C^{L0}_{l0l'0} = 0$ for odd values of the sum $L = l+l'$. In the context of NC-beams, this would be a handicap if reflection symmetry is violated leading to odd-parity BipoSH coefficients (see Sec. III). Also it is blind to a number of other interesting possibilities with odd-BipoSH signals.